UNIVERSITEIT VAN PRETORIA
UNIVERSITY OF PRETORIA
YUNIBESITHI YA PRETORIA

Locating Resonances in a Complex Potential Field

B H S J Fakira-Du Toit

October 2016

Abstract

Locating Resonances in a Complex Potential Field

by

Hamida Fakira

Supervisor:	Professor S Rakityansky
Degree:	*MSc Physics*
Keywords:	Resonance,Jost Function,Complex Absorbing Potential

The main question that has been answered in this research project is: what happens to the singularities of the S-matrix when the interaction potential becomes complex? In other words, we looked at the resonance spectral points and traced their movements on the complex momentum plane, when the imaginary part of the potential is gradually increased from zero to a certain reasonable value. This question is important in many fields of research where optical potentials are used. An optical potential can effectively take into account the loss of the beam of particles into all the reaction channels that are formally ignored. Such a simplified approach is widely used in nuclear and atomic physics. In order to study the movement of the spectral points, we used a simple potential and the Jost function method that allowed us to easily locate the spectral points as complex zeros of the Jost function.

Declaration

I, *Hamida Fakira* declare that the dissertation, which I hereby submit for the degree *MSc Physics* at the University of Pretoria , is my own work and has not previously been submitted by me for a degree at this or any other tertiary institution.

Signature:	.... Hamida Fakira
Student number:	28680040
Date:	December 20, 2016

Acknowledgement

I wish to extend my sincere gratitude to the following people and institutions for their contribution to this dissertation:

- My supervisor, Professor S Rakityansky, and fellow students for their assistance, guidance and encouragement throughout the study.
- My family and friends for their faith in my abilities, continuous support and encouragement.
- I would also like to thank Louwrens van Schalkwyk at the Department of Physics, at the University of Pretoria for putting this LaTeX 2_{ε} template together.

Dedication

To Shaaiqah and Riyazah who gave me a sense of purpose, against all odds.

Contents

List of Figures

1 Introduction

Resonance was discovered by Galileo Galilei, during his investigations of pendulums and musical strings in 1602. The vibrations or oscillations of systems constitute one of the most important fields of study in physics. Virtually every system possesses the capability for vibration, and most systems can vibrate freely in a large variety of ways.

As Bishop puts it:

> "After all, our hearts beat, our lungs oscillate, we shiver when we are cold, we sometimes snore, we can hear and speak because our eardrums and larynges vibrate. The light waves which permit us to see entail vibration. We move by oscillating our legs. We cannot even say 'vibration' properly without the tip of the tongue oscillating...Even the atoms of which we are constituted vibrate." [1]

In classical physics, the phenomenon of resonance occurs when a system is made to 'vibrate'at a driving frequency that is close to its natural frequency of vibration. Then, the amplitude of oscillation becomes very large by repeated application of a relatively small force. [2]

In a classical example of 'mass and spring' system, the system is acted upon by an external agent, one parameter of which (the frequency) is varied. The response of the system, as measured by its amplitude and phase, or by the power absorbed, undergoes rapid changes as the frequency passes through a certain value. The form of the response is described by two quantities: a resonance frequency, and a width, which characterise the distinctive properties of the driven system.

Resonance is the phenomenon of driving the system under such conditions that the interaction between the driving agent and the system is maximised. The interaction has its maximum at or near the natural frequency. [2]

Resonance phenomena occur whenever vibrations or waves or periodic motion occurs. There is mechanical resonance, acoustic resonance, electromagnetic resonance, nuclear magnetic resonance (NMR), electron spin resonance

(ESR),etc.

In classical physics, a particle is *well localised* in space, because its position and velocity can be measured simultaneously with precision. Within the context of quantum mechanics, quantum particles display both particle and wave features (wave-particle duality). A quantum particle is described by a *wave function*, $\boldsymbol{\Psi}$ corresponding to the matter wave associated with the particle. The quantum particle exhibits the de Broglie wave relation of $\boldsymbol{E} = \hbar\boldsymbol{\omega}$ which describes the relationship between the energy $\boldsymbol{E}$ and the circular frequency $\boldsymbol{\omega}$, and $\hbar$ which is the Planck constant [3].

The wave function of a quantum particle is generally denoted as $\boldsymbol{\Psi(E, \vec{r})}$, indicating that it is a function of energy $\boldsymbol{E}$ and position $\boldsymbol{\vec{r}}$. Whilst in classical mechanics, resonance refers to a state when the system vibrates with maximum amplitude, in quantum mechanics, **resonance is a phenomenon of localizing $\boldsymbol{\Psi(E, \vec{r})}$ for a certain time interval**. In other words, the particle stays within a certain defined volume of space longer than expected, instead of simply passing by. Indeed, the propagation of a wave packet in the presence of a resonance experiences a time delay [33].

Radioactive decay is an example or instance of a temporarily localized quantum particle, or, of a particle **decaying from quantum resonance**. A quantum resonance is a quasi-stationary or quasi-bound states and have a finite lifetime. When resonance is formed, energy (of the unstable quantum particle) is rapidly distributed among all possible degrees of freedom and the quantum particle *forgets* how it entered into the resonance. This means that there is no preferred direction for its decay. It further implies that the information contained in the incoming wave (before it entered into resonance) is forgotten. This principle forms the basis of the mathematics to locate a resonance or determine when a resonance will occur [6]. Mathematically, this fact implies that the asymptotics of the wave function only has the outgoing wave.

An instance of a resonance decaying isotropically can be observed in the case of a sample of Polonium atoms $^{\mathbf{212}}$Po. The nuclei of these atoms can be viewed as quasi-bound states of $^{\mathbf{208}}$Pb and $\boldsymbol{\alpha}$-particles. During the decay process,these $\boldsymbol{\alpha}$-particles are emitted randomly in all directions with a uniform distribution. It is an isotropic decay.

Quantum resonance decays stochastically according to the radioactive law;

$$N = N_0 \exp\left(-\Gamma t/\hbar\right) \quad ,$$

where, N_0 is the number of particles in an initial ensemble of quantum particles,
N is the number of particles at time t,
Γ is the resonance width and is measured in the units of energy. It is commonly known as the *decay rate.*

The time dependent wave function Ψ of the quantum particles that constitute the ensemble N_0 can be expressed as:

$$\Psi(\vec{r},t) = \Psi(\vec{r}) \exp\left(\frac{-i}{\hbar}Et\right)$$

Note that the space distribution of the probability does not depend on time, if the energy E is real. Indeed the probability density is given by [3]:

$$|\Psi(\vec{r},t)|^2 = \Psi^*(\vec{r},t)\Psi(\vec{r},t) = |\Psi(\vec{r})|^2$$

In order to satisfy the radioactive law of decay, the time dependent wave function of the particle, Ψ, must be proportional to $\exp\left(-\Gamma t/2\hbar\right)$. This requirement is fulfilled when the energy E has a negative imaginary part, given as;

$$E = E_r + E_i \quad \text{where} \quad E_i = -i\Gamma/2$$

$$\text{then} \quad E_{resonance} = E_r - i\Gamma/2$$

$$\text{and} \quad \Psi(\vec{r},t) = \Psi(\vec{r}) \exp\frac{-i}{\hbar}(E_r - i\Gamma/2)t$$

Quantum resonances, similar to bound states,are spectral points. Spectral points are certain discrete points in the complex energy $E-$ plane, at which the physical wave function has only outgoing waves in its asymptotic behaviour (i.e, how the wave behaves as $r \to \infty$). The bound, resonant and virtual states are spectral points on the $E-$ plane [15]. The energies of quantum resonances are however complex eigen values [8]. The imaginary part Γ determines how fast the resonance decays or the duration the particle stays localized. The half-life of the quantum resonance is given as

$$\tau_{1/2} = \frac{\hbar \ln 2}{\Gamma}$$

The bigger the value of $\mathbf{\Gamma}$, the smaller the half-life, i.e., the faster the decay. The half-life of nuclear decay varies greatly across the spectrum of atoms. The $^{\mathbf{14}}$C has a half-life of 5730 years whilst a muon particle $\boldsymbol{\mu}^{+}$ has a lifetime of $\mathbf{2.2}$x$\mathbf{10^{-6}}$ seconds. $^{\mathbf{218}}$Po decays through $\boldsymbol{\alpha}$-emission with a half-life of 3.1 minutes to $^{\mathbf{214}}$Pb, whilst the newly created lead particle decays through $\boldsymbol{\beta}$-emission to $^{\mathbf{214}}$Bi with a half-life of 27 minutes [7].

The temporary localization of a quantum particle, i.e, quantum resonance, can be visualised in terms of a particle moving towards a centre of force with such a kinetic energy that its trajectory around the centre is almost closed. As a result it does many revolutions around the centre before moving away. The more revolutions it does, the longer the resonance ***lives***. From a quantum mechanical perspective, the particle forms a partially localized state which slowly leaks out [9].

Resonances are characterised by discrete values of resonant frequency at which energy is accumulated in small region of space. The frequency window around the discrete energy values, are known as the resonance width or $\mathbf{\Gamma}$. The accumulated energy leaks out through the window. Narrow resonances are most pronounced and visible in experiment because the frequency window or alternatively known as resonance widths, are narrow. The leakage of energy is thus slower than in the case of broad resonances. This means that narrow resonances live longer than broad resonances.

Let us consider an experiment in which a ’particle’ is scattered from a ’target’. The *’particle’* can be, for example, an electron, a nucleon, an atom or a molecule. The *’target’* can be a nucleus, an atom, a molecule, a flat or corrugated solid surface. In an elastic scattering experiment the energy of the ’particle’ is conserved. In a non-elastic scattering experiment there is an energy exchange between the ’particle’ and the intrinsic degrees of freedom of the ’target’. Also the final energy of the ’particle’ in its ’out’ asymptote limit can be smaller or larger than the initial energy of the ’particle’ in its ’in’ asymptote limit. In a reactive scattering experiment the ’particle’ and the ’target’ undergo a change during the re-arrangement collision and become different species. Two possibilities of scattering exist [12].

(i) Figure 1(a) illustrates a direct scattering event.

(ii) Figure 1(b) illustrates the second possibility, where, due to multiple-scattering events, the particle is temporarily trapped by the target.

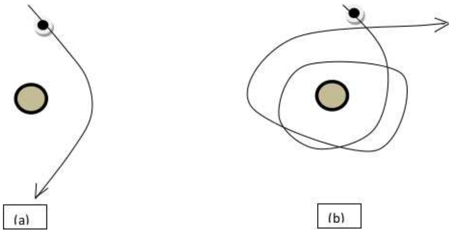

Figure 1: Two Different possible Scattering Orbits

> When the lifetime of the particle-target system in the region of interaction is larger than the collision time in a direct collision process, this phenomenon is called a resonance phenomenon.

Thus, a resonance state can also be defined as a long-lived state of a system which has sufficient energy to break-up into two or more subsystems. The subsystems are associated with the scattering particle and the target [12].

In scenario 1(b), before moving apart, the 'particle' and the 'target' stay together for a while. During the resonance lifetime, the 'particle' move around the 'target' and 'forget' the direction from which it came [13]. When the resonance eventually decays, the particle 'chooses' the direction to move away at random. In quantum mechanics, this physical concept is mathematically formulated. The resonant states are spectral points, i.e, the eigenstates of the Hamiltonian,

$$\boldsymbol{H\Psi = E\Psi}$$

with **pure outgoing wave asymptotics and no 'memory' of the incoming information**.

In the system described above of a particle moving towards a centre in a circular orbit, the wave function describing the resonance state obeys the differential Schrödinger equation, in spherical coordinates:

$$\boldsymbol{\left\{\partial_r^2 + k^2 - \frac{l(l+1)}{r^2}\right\}\Psi_l(k,r) = V(r)\Psi_l(k,r)}$$

where $\boldsymbol{k}$ is the wave number [11]. The general solution for this differential equation asymptotically behaves as:

$$\boldsymbol{\Psi_l(k,r) \underset{r\to\infty}{\longrightarrow} f_l^{(in)}(k)h_l^{(-)}(kr) + f_l^{(out)}(k)h_l^{(+)}(kr)}$$

where $\boldsymbol{h_l^{(\pm)}(kr)}$ are the Riccati-Hankel functions. $\boldsymbol{h_l^{(-)}(kr)}$ represents the incoming spherical wave and $\boldsymbol{h_l^{(+)}(kr)}$ is the outgoing spherical waves. The functions $\boldsymbol{f_l^{(in)}}$ and $\boldsymbol{f_l^{(out)}}$ are the amplitudes of the corresponding waves. They depend on the total energy and vary with the angular momentum $\boldsymbol{\ell}$. [16]

Based on the physical concept that the particle *does not remember* how it entered into a resonance state, mathematically, it means that the coefficient of the incoming wave should be zero, that is;

$$\boldsymbol{f_l^{(in)}(k) = 0}$$

This coefficient is commonly referred to as the *Jost function*. Siegert applied this mathematical approach to obtain scattering resonance positions as far back as 1939 [6]. Resonances therefore correspond to spectral points of $\boldsymbol{E_{resonance}}$ which are complex and at which the Jost function of the incoming wave is effectively zero. This is the concept on which this dissertation is premised.

Several techniques have been developed by scientists over the years for locating resonances for various potential models. The objective of most studies is to increase the accuracy of values obtained and to improve the computational efficiency in locating resonances. There are two sets of methods for investigating the location of the resonances:

- Directly in the complex energy plane or complex momentum k plane, since
$$\boldsymbol{k^2 = \frac{2m}{\hbar^2}(E)}$$
- Indirectly by analyzing the scattering data at real energies.

Using the direct method, the resonance can be located by finding the zeroes of the Jost function [14].

The direct method is premised on the fact that the energy spectrum of the Hamiltonian consists of three parts [13]:

- A discrete set of real points on the negative energy axis corresponding to the bound states,
- Real positive energy line corresponding to the continuum scattering states,
- A discrete set of points in the lower half of the complex energy plane corresponding to the resonance states.

The third part are quasi-stationary/resonant states that are unstable, decaying at a rate that increases with the negative value of the imaginary part of the resonance energy (i.e. $\boldsymbol{\Gamma/2}$).

In this dissertation, we use the direct method and trace the location of the resonance on the complex momentum k plane. We start with the second order differential radial Schrödinger equation in spherical coordinates. The asymtotic behaviour (as $\boldsymbol{r} \rightarrow \infty$) of the radial wave function $\boldsymbol{u_l}$*(k,r)*, indicates that it behaves as a linear combination of the Riccati-Hankel functions. By applying the variation parameters methods and the Lagrange condition [10] , the second order Shrödinger equation is transformed into a coupled system of first order differential equations for the Jost functions. The Jost functions are, as explained previously, amplitudes in the asymtotics of the radial wave function. A numerical solution is used to solve the coupled differential equations and to calculate the values of the complex momentum k that result in the Jost function being zero. These zeroes determine the location or presence of resonances. On the $\boldsymbol{k}-$ plane, the resonances are spectral points that are located in the fourth quadrant, i.e., negative imaginary $\boldsymbol{k}$ values and positive real $\boldsymbol{k}$ values.

The boundary behaviour of the radial wave function from $\boldsymbol{r = 0}$ at the centre of the spherical potential, to $\boldsymbol{r}$ at large distances are critical in determining the solution to the coupled first order differential equations. Within the spherical boundary under consideration, we assume that the wave function $\boldsymbol{u_l}$ *(k,r)* must be zero at $\boldsymbol{r = 0}$. In the case of a finite-range potential, it is assumed that the potential vanishes to zero at large enough $\boldsymbol{r}$. Then, the Jost functions can be accurately determined. The energy parameter, in these differential equations, can be set to any complex value, as required at resonance.

Thus, using certain boundary conditions, it appears to be simple enough to determine the zeroes of the Jost functions and hence to locate the resonances. However, in reality, we are confronted with two main challenges in this approach.

- **The first challenge** is the asymptotic behaviour of the interacting potential. In real life the potential does not simply vanish to zero as the particle moves to infinity.

  Realistic potentials have tails extending to infinity. In such cases, the solutions to the coupled differential equations do not always converge to the corresponding Jost functions. The zeroes of the Jost functions cannot be accurately determined and thus, the resonant wave seems to diverge to infinity.

  Realistic potentials are usually divided into two classes, the short-range and long-range potentials. The short-range potentials tend to vanish exponentially or faster at infinity. In our dissertation we have used a potential that vanish at infinity faster than the Coulomb potential (i.e $\boldsymbol{V(r) = (-e^2)/r}$).

- **The second challenge** arises from the fact that the scattering event usually results into non-conservation of the probability density of the wave function. The probability density is not conserved because of a loss of flux. What happens generally is that the scattering event results in a major outcome plus some sub-outcomes (or subsystems) that account for the loss of flux or particles *before the event* not being exactly the same as to what is emitted *after the event*. Each outcome can be described by a particular set of partial wave *channel*. Hence the event is known as a multi- channel interaction when multiple outcomes occur.

To resolve the problem that as $\boldsymbol{r \to \infty}$ the potential does not abruptly cut off (i.e, the first challenge explained above), the common approach is the:

- **Complex Coordinate Rotation** method also known as complex scaling method (CSM). In this method the coordinates of the system are

> rotated in the complex coordinate (momentum) plane. After the complex rotation,the resonance wave function is damped in the asymptotic region and the complex eigen value gives the resonance parameters $\boldsymbol{E_r}$ and $\boldsymbol{\Gamma/2}$ (the resonance energy and the decay width).

To account for the change or loss in flux subsequent to a scattering event, that leads to resonance, the most suitable potential that can mathematically model the interaction between, say two nuclei, is one that has a negative imaginary as well as a real component [33]. The mathematical implication of the imaginary component of the potential $\boldsymbol{V(r)}$ is described below.

In general, quantum particles interaction is given by the Shrödinger equation;

$$(\hat{\boldsymbol{T}} + \hat{\boldsymbol{V}})\boldsymbol{\Psi} = \boldsymbol{i\hbar}\frac{\boldsymbol{\partial\Psi}}{\boldsymbol{\partial t}}$$

where, $\hat{\boldsymbol{V}}$ represents the effective interacting potential.

If the interacting potential is purely real, then it accounts only for those events where total probability density is conserved. In nature, however, there are more reactions occurring, leading to loss in conservation of probability density. Such reactions remove flux from elastic scattering. This removal can be equivalently modelled using complex potentials. The imaginary component of the potential can also model actual interactions that reproduce resonances that diverge. The potentials that fit or best model elastic scattering are therefore generally complex.

If the potential is $\boldsymbol{V(r) + iW(r)}$ and the imaginary part $\boldsymbol{W < 0}$, then it is an *absorptive potential.* It accounts for the loss of flux during a scattering event or an interaction between two or more particles.

Potentials with both real and imaginary components are also referred to as optical potentials since they describe both the refraction and the absorption, (that occurs during a scattering event) in the same way as a light wave passing through a cloudy refractive medium.

The Shrödinger equation is then written as;

$$(\hat{\boldsymbol{T}} + \boldsymbol{V} + \boldsymbol{iW})\boldsymbol{\Psi} = \boldsymbol{i\hbar}\frac{\boldsymbol{\partial\Psi}}{\boldsymbol{\partial t}}$$

where it has an imaginary potential W. The rate of loss of flux is then calculated as;

$$\frac{\partial \Psi \Psi^*}{\partial t} = -\vec{\nabla} \cdot \vec{j} + \frac{2}{\hbar} W \Psi \Psi^*$$

where j is the flux or nuclear probability current.

As $W < 0$, the imaginary potential effectively acts as a *sink* of particles. The imaginary potential accounts for the loss of flux that occurs in a scattering event. The effective complex potential $V + iW$ is also referred to as the *complex absorbing potential* [33].

In this project, initially, we use a purely real central potential, $V(r)$. The coupled differential equation is solved numerically to locate the zero of the Jost function. A negative imaginary component is then added to the potential. The value of the imaginary component is increased gradually. For each value of the imaginary component the corresponding values of the complex momentum k, where the Jost function is zero, is calculated. These are then plotted on the complex k plane. Thus, we obtain a trajectory of resonances in the fourth quadrant of the complex $k-$ plane.

Since,

$$k^2 = \frac{2\mu E}{\hbar^2}$$

it implies that

$$E = \frac{\hbar^2}{2\mu}\left\{(Rek)^2 - (\mathrm{Im}\ k)^2 + 2i(Rek)(Imk)\right\}$$

The values of the resonant energy E can then be calculated as well as the imaginary part of the energy which is given as;

$$E_i = 2i(Rek)(Imk)$$

Knowing that $E_i = -\Gamma/2$, the resonance width Γ can be calculated. Thus we are able to observe the trend in the width of the resonance as the imaginary component W or $\mathrm{Im}\, V$ becomes more negative. The observation is that the spectral points or resonances move further away from the real-k axis towards the negative imaginary-k axis. That is, as the imaginary component of the potential becomes more negative, sub-threshold resonances are observed.

The results correspond to those found elsewhere in the literature. [15] [18] [9].

This report is organised as follows. In the first section, we explain the theoretical relationship between the complex momentum $\boldsymbol{k}$ and the complex energy $\boldsymbol{E}$ when a particle is subjected to a spherical central potential. We elaborate on how different energy eigen values, result in the quantum particle being in one of three different states, namely,the bound state, the scattering state and the resonance state. The asymptotics or boundary conditions that satisfy the Shrödinger radial equation for each of these states are described.

In the second section we apply the variation parameters method for transforming the radial Schroedinger equation, into a coupled first order linear differential equations of the Jost functions. The asymptotic behaviour of the short-range potential in the determination of the zeroes of the Jost function is explained. We also determine the limit of convergence of the Jost function on the complex $\boldsymbol{k}-$ plane.

In the third section, we explain the mathematical implications of the imaginary component of a potential, its impact on the divergence of the resonance wave and the actual complex potential that has been chosen for this project research. The coupled differential equation is then solved numerically using an iterative computation to determine the zeroes of the Jost function. The results of the computation are presented graphically and thus, we demonstrate the trajectory of the resonance spectral points (that is, zero of Jost function) as the imaginary component of the potential is decreased incrementally, on the complex $\boldsymbol{k}-$ plane. Broader resonances (spectral points are located further away from the real positive $\boldsymbol{k}-$ axis) are obtained as the imaginary component of the potential decreases.

In the final section, the significance of the trajectory of the resonance spectral points are explained and compared with previous theses. We then give an overview of instances where the complex absorbing potential approach of locating resonances can be utilised.

2 Quantum States

In quantum mechanics, a state of a physical system is completely described by the wave function $\boldsymbol{\Psi}$ obeying the Schrödinger equation:

$$\boldsymbol{E\Psi} = \boldsymbol{\hat{H}\Psi} \tag{1}$$

It generally relates to standing waves called stationary states (also known as 'orbitals' as in atomic orbitals or molecular orbitals). The equation describes stationary states of any quantum particle (i.e., could be proton, neutron,or electron).

Let us consider the motion of a particle of mass $\boldsymbol{\mu}$ moving under the influence of a potential $\boldsymbol{V}$. In the coordinate representation, equation (2) reads:

$$\boldsymbol{E\Psi(\vec{r})} = \left[\frac{-\hbar^{\mathbf{2}}}{\mathbf{2}\boldsymbol{\mu}}\boldsymbol{\nabla}^{\mathbf{2}} + \boldsymbol{V(\vec{r})}\right]\boldsymbol{\Psi(\vec{r})} \tag{2}$$

where:
$\hbar = \mathbf{1.05459}$ x $\mathbf{10}^{(\mathbf{-34})}$ J·s and it is the Planck's constant,
$\boldsymbol{\nabla}^{\mathbf{2}}$ is the Laplace operator, and
$\boldsymbol{\Psi(\vec{r})}$ is the wave function of the particle, defined over space.

The wave function $\boldsymbol{\Psi}$ contains all the information about a particle or quantum system.

2.1 The Three Dimensional Schrödinger Equation

In a three dimensional problem, using the spherical coordinates, the Laplacian operator $\boldsymbol{\nabla}^{\mathbf{2}}$ or $\triangle$, has the form;

$$\triangle = \frac{\mathbf{1}}{\boldsymbol{r}^{\mathbf{2}}}\frac{\boldsymbol{\partial}}{\boldsymbol{\partial r}}\left(\boldsymbol{r}^{\mathbf{2}}\frac{\boldsymbol{\partial}}{\boldsymbol{\partial r}}\right) + \frac{\mathbf{1}}{\boldsymbol{r}^{\mathbf{2}}\,\mathbf{sin}\,\boldsymbol{\theta}}\frac{\boldsymbol{\partial}}{\boldsymbol{\partial\theta}}\left(\mathbf{sin}\,\boldsymbol{\theta}\frac{\boldsymbol{\partial}}{\boldsymbol{\partial\theta}}\right) + \frac{\mathbf{1}}{\boldsymbol{r}^{\mathbf{2}}\,\mathbf{sin}^{2}\,\boldsymbol{\theta}}\frac{\boldsymbol{\partial}^{\mathbf{2}}}{\boldsymbol{\partial\varphi}^{\mathbf{2}}} \tag{3}$$

where, the spherical angles $\boldsymbol{\theta}$ is the polar coordinate with $\boldsymbol{\theta} \in [\mathbf{0}, \boldsymbol{\pi}]$ and, $\boldsymbol{\varphi}$ is the azimuthal coordinate with $\boldsymbol{\varphi} \in [\mathbf{0}, \mathbf{2}\boldsymbol{\pi}]$.
Figure below shows the relationship between $\boldsymbol{\theta}$, $\boldsymbol{\varphi}$ and $\boldsymbol{r}$ [28].

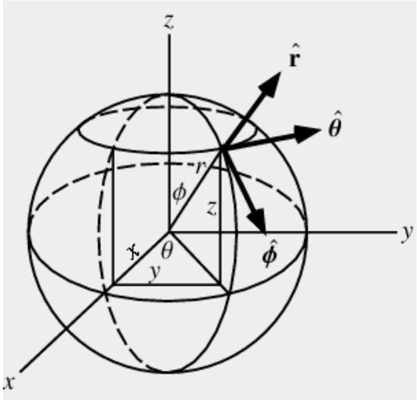

Figure 2: Spherical Coordinates

Inserting (3) into equation (2), the three dimensional Schrödinger equation in spherical coordinates can be expanded as:

$$\boldsymbol{E\Psi(r,\theta,\varphi)} = \frac{-\hbar^2}{2\mu}\left[\frac{1}{r^2}\frac{\partial}{\partial r}(r^2\frac{\partial}{\partial r}) + \frac{1}{r^2\sin\theta}\frac{\partial}{\partial\theta}(\sin\theta\frac{\partial}{\partial\theta}) + \frac{1}{r^2\sin^2\theta}\frac{\partial^2}{\partial\varphi^2}\right]\Psi(r,\theta,\varphi) + V(r)\Psi(r,\theta,\varphi) \quad (4)$$

The wave function $\boldsymbol{\Psi}$ can generally be expressed as:

$$\boldsymbol{\Psi(\vec{r},\theta,\varphi)} = \sum_{\ell m} \boldsymbol{R_\ell(r)Y_{\ell m}(\theta,\varphi)}$$

where,
$\boldsymbol{R_\ell(r)}$ is the radial part of the wave function,
$\boldsymbol{Y_{\ell m}(\theta,\varphi)}$ is the angular part of the wave function.

Replacing the unknown function $\boldsymbol{R_\ell(r)}$ with the function $\boldsymbol{u_\ell(r)}$ via the relationship $\boldsymbol{R_\ell(r) = u_\ell(r)/r}$ and, using the method of separation of variables, the equation (4) can be decomposed into $\boldsymbol{r}$, $\boldsymbol{\theta}$ and $\boldsymbol{\varphi}$ [28].

Denoting

$$\boldsymbol{U(r)} = \frac{2\mu}{\hbar^2}\boldsymbol{V(r)}$$

for the radial part of the wave function in (4), we obtain:

$$-\frac{\mathrm{d}^2 u_\ell(r)}{\mathrm{d}r^2}+\left[U(r)+\frac{\ell(\ell+1)}{r^2}\right]u_\ell(r)=\frac{2\mu}{\hbar^2}Eu_\ell(r) \tag{5}$$

The energy and momentum are related to each other in the same way as in classical mechanics, that is,

$$E=\frac{p^2}{2\mu}$$

In quantum mechanics, it is more convenient to use the so-called wave vector $\vec{k}=\hbar\vec{p}$, for which this relation gives

$$k^2=\frac{2\mu}{\hbar^2}E$$

k is also known as the dimensionless momentum and it corresponds to the 'shifted' energy.

Equation (5) can be further simplified to

$$\left\{\frac{\mathrm{d}^2}{\mathrm{d}r^2}+k^2-\left[\frac{\ell(\ell+1)}{r^2}+U(r)\right]\right\}u(r)=0 \tag{6}$$

where $\ell(\ell+1)/r^2$ is analogous to the centrifugal potential of classical mechanics.

The centrifugal potential is a repelling force that is associated with orbital angular momentum and it repels the particle away from the spherical centre. It is called the centrifugal barrier. Since the variable r can take on non-negative real values only, the centrifugal potential is always positive or zero [3].

2.2 Asymptotic Behaviour

It is important to understand how both the radial wave function $u_\ell(r)$ and the potential $U(r)$ behave as the particle moves towards the centre, that is, $r \to 0$ as well as when the particle drifts away from the centre, that is, $r \to \infty$.

2.2.1 Radial wave behaviour as $r \to 0$

The radial wave function $R_\ell(r)$ is a physical wave that has to be finite everywhere. Since $R_\ell(r) = u_\ell(r)/r$, then at the origin where $r = 0$, $u_\ell(r)$ must vanish, i.e., $u_\ell(0) = 0$ at the origin.

For very small values of r, we can assume that the potential $U(r)$ is less singular than the centrifugal potential, i.e,

$$\lim_{r \to 0} r^2 U(r) = 0$$

then the equation (6) reduces to

$$\frac{\mathrm{d}^2 u_\ell(r)}{\mathrm{d}r^2} + k^2 u_\ell(r) - \frac{\ell(\ell+1)}{r^2} u_\ell(r) \simeq 0 \qquad \text{as} \qquad r \to 0$$

whose solution is of the form;

$$u_\ell(r) = A r^{\ell+1} + B r^{-\ell}$$

where A and B are constants.

Since $u_\ell(r)$ vanishes at $r = 0$ whilst the second term $r^{-\ell}$ diverges at $r = 0$, the latter has to be discarded. Hence, for small values of r, the solution is [3];

$$u_\ell(r) \xrightarrow[r \to 0]{} const \cdot r^{\ell+1}$$

2.2.2 Potential as $r \to 0$

In order to distinguish the reasonable potentials from the unreasonable ones (e.g., where the attraction is so strong that the particle falls deep into the spherical potential well), we consider possible restrictions on the behaviour of the potential.

Suppose the potential behaves near the centre as;

$$V(r) \xrightarrow[r\to 0]{} -\frac{\alpha}{r^s}, \qquad \text{where} \qquad \alpha > 0.$$

If we look at a wave function that is finite in a small sphere of radius r_o around the centre and is zero outside of this sphere, then it is located near the point $r = 0$ with an uncertainty $\triangle r \sim r_o$.

The corresponding uncertainty of the momentum is thus [27],

$$\triangle p \sim \hbar / r_o$$

And the total energy is;

$$< E >=< E_{kin} > + < V >\sim \frac{\hbar^2}{2\mu r_o^2} - \frac{\alpha}{r_o^s} \tag{7}$$

Note that

- $< E_{kin} >$ is positive
- $< V >$ is negative

This indicates that the total energy $< E >$ can be either $+\infty$ or $-\infty$, as $r_o \to 0$. There are three possibilities that depend on whether the exponent s is; $s > 2$ or $s < 2$ or $s = 2$

As can be seen from (7), the fall onto the centre (i.e. $< E >= -\infty$) can be avoided only if $s < 2$.

This means that the physical potentials are those potentials that are less singular at the origin than $1/r^2$. It should be noted, however, that this conclusion is only valid for an attractive potential. Equation (7) shows that for a repulsive potential, the value of s can be anything.

2.3 The Free Radial Schrödinger Equation

In the instance where the potential $\boldsymbol{V(r) = 0}$, and equation (6) becomes the **'free'** radial Schrödinger equation:

$$\left\{\frac{\mathrm{d}^2}{\mathrm{d}r^2} + k^2 - \frac{\ell(\ell+1)}{r^2}\right\} u_\ell(r) = 0 \tag{8}$$

The solutions to the free radial Schrödinger (8) are the so-called Riccati-Bessel, Riccati- Neumann and Riccati-Hankel functions;

$$j_\ell(kr) \qquad \text{and} \qquad n_\ell(kr) \qquad \text{and} \qquad h_\ell^{(\pm)}(kr)$$

where $h_\ell^{(\pm)}(kr) = j_\ell(kr) \pm i n_\ell(kr)$

At large distances, the Riccati-Hankel functions, independently of the value of the angular momentum, behave exponentially [27];

$$h_\ell^{(\pm)}(kr) \underset{r\to\infty}{\longrightarrow} \mp i \exp[\pm i(kr - \ell\pi/2)] \tag{9}$$

When $\boldsymbol{\ell = 0}$, the solution to equation (8) are the well-known trigonometric functions;

$$\sin(kr) \qquad \text{and} \qquad \cos(kr) \qquad ,$$

which are particular cases of the Riccati-Bessel and Riccati-Neumann functions.

As can be seen from equation (9), the functions $h_\ell^{(-)}(kr)$ and $h_\ell^{(+)}(kr)$ describe the in-coming and out-going spherical waves, respectively.

2.4 Jost Functions in the Schrödinger Solution

In the case where the potential $\boldsymbol{V(r)}$ is present, the radial Schrödinger equation is,

$$\left[\frac{d^2}{dr^2} + k^2 - \frac{\ell(\ell+1)}{r^2}\right] u_\ell(E,r) = V(r)u_\ell(E,r) \tag{10}$$

The above equation can be solved using the method of variation of parameters as described in the theory of ordinary differential equation [36]. Let us write the unknown radial wave function as:

$$u_\ell(E,r) = h_\ell^{(-)}(kr)F_\ell^{(in)}(E,r) + h_\ell^{(+)}(kr)F_\ell^{(out)}(E,r) \tag{11}$$

where; $F_\ell^{(in/out)}(E,r)$ are unknown functions of energy E and position r. At large distances (i.e., $r \to \infty$), where the potential disappears, equation (10) becomes the "free" Shrödinger equation. As we have seen in Section (2.3), its two independent solutions are the Riccati- Hankel functions. Any other solution is their linear combination.

Therefore,

$$u_\ell(E,r) \underset{r\to\infty}{\longrightarrow} h_\ell^{(-)}(kr)f_\ell^{(in)}(E) + h_\ell^{(+)}(kr)f_\ell^{(out)}(E) \tag{12}$$

where

$$f_\ell^{(in/out)}(E) = \lim_{r\to\infty} F_\ell^{(in/out)}(E,r)$$

The coefficients $f_\ell^{(in)}(E)$ and $f_\ell^{(out)}$ indicate the type of quantum state, the particle can be found. The particle can be in either bound, scattering or resonance state. These coefficients depend on the energy of the system and vary with the momentum k.

These coefficients are called the **Jost functions**. In equation (12), the function $h_\ell^{(-)}(kr)$ represents the incoming wave and $f_\ell^{in}(E)$ is its amplitude, $h_\ell^{(+)}(kr)$ represents the outgoing wave and $f_\ell^{out}(E)$ is the amplitude of the outgoing wave.

2.5 Jost Function and the Bound State

In physics, a bound state is the state of a system where a particle is subject to a potential such that the particle remains localized in one or more regions of space. The potential may be either an external potential or the result of the presence of another particle.

In quantum mechanics, a bound state is a state in Hilbert space that corresponds to two or more particles whose interactive or joint energy is less than the total energy of each separate particle, and thus, these particles cannot be separated unless energy is spent.

Examples of bound states are:

1. A proton and an electron can move separately. The total centre of mass energy is positive and such a pair of particles can be described as ionized atom. Once the electron starts to 'orbit' the proton, the energy becomes negative and a bound state, namely the hydrogen atom, is formed.
2. A nucleus is a bound state of protons and neutrons commonly called nucleons.
3. A positronium 'atom' is an unstable bound state of an electron and a positron. It decays into photons because of the e^+e^- annihilation.

In a bound state, a particle cannot leave the source of the attractive field. The probability density wanes when $r \to \infty$ and $u_l(E, r) \to 0$
Since the total probability of finding the particle somewhere around the source of potential is 1, then

$$\int |\psi(\vec{r})|^2 d\vec{r} = 1$$

If we choose the energy scale in such a way that the energy at infinite r is zero, it means that the energy decreases from zero at infinity to the bound states. That is, the **bound states have negative energies** and thus, the momentum k is imaginary since,

$$k = \sqrt{\frac{-2\mu}{\hbar^2}|E|} = i\kappa \quad , \quad \kappa > 0$$

Since, in a bound state,

$$\boldsymbol{u_\ell(E,r)} \underset{r\to\infty}{\to} \mathbf{0} \tag{13}$$

Comparing equation (13) with equation (12), the radial wave function vanishes to zero, depending on the asymptotic behaviour of the Riccati functions and Jost coefficients.

As $\boldsymbol{r \to \infty}$, the Riccati-Hankel functions with pure imaginary $\boldsymbol{k = i\kappa}$ behave in a way that the one term grows exponentially while the other vanishes, i.e.,

$$\boldsymbol{h_\ell^{(+)}(kr)} \underset{r\to\infty}{\to} \mathbf{exp}\,\boldsymbol{(-\kappa r)} \qquad \text{as} \qquad \boldsymbol{r \to \infty} \qquad \boldsymbol{h_\ell^{(+)}(kr) \to 0}$$

$$\boldsymbol{h_\ell^{(-)}(kr)} \underset{r\to\infty}{\to} \mathbf{exp}\,\boldsymbol{(\kappa r)} \qquad \text{as} \qquad \boldsymbol{r \to \infty} \qquad \boldsymbol{h_\ell^{(-)}(kr) \to \infty}$$

This implies that in equation (12), only the second term can survive for a bound state,i.e.,

$$\boldsymbol{u_\ell(E,r)} \underset{r\to\infty}{\longrightarrow} \boldsymbol{h_\ell^{(+)}(kr) f_\ell^{out}(E)} \tag{14}$$

This bound state condition may be achieved at certain discrete points, $\boldsymbol{E < 0}$ that are roots of the equation $\boldsymbol{f_\ell^{in}(E) = 0}$.

This correlates with the theory that the amplitude of the incoming wave is zero as $\boldsymbol{r \to \infty}$. Since the amplitude of the incoming wave is given as $\boldsymbol{f_\ell^{(in)}(E)}$, by calculating $\boldsymbol{f_\ell^{(in)}(E) = 0}$, that is, by determining the zero of the Jost function, the bound state can be located.

On an energy plane or $\boldsymbol{k}$-plane, bound states correspond to the points where the Jost functions $\boldsymbol{f_\ell^{(in)}}$ are zeroes that is, where the physical wave function has only outgoing waves in its asymptotic behaviour. The energies of the bound state are negative and the corresponding momentum $\boldsymbol{k}$ are imaginary.

The discrete points where the Jost function is zero are called the spectral points. Figure (3) shows the location of the bound states on the $\boldsymbol{k}$ and $\boldsymbol{E}$ planes.

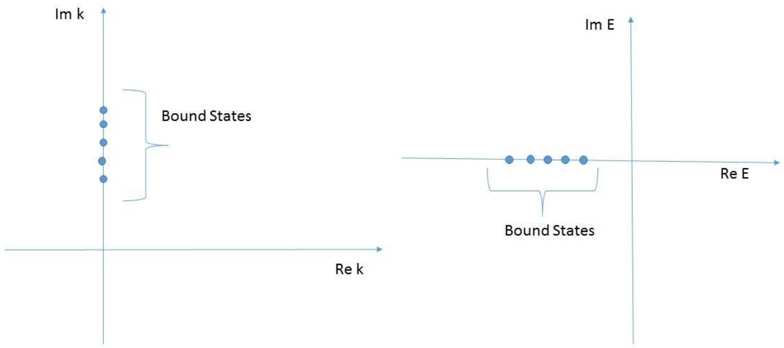

Figure 3: Bound States on $\boldsymbol{k}$ plane and $\boldsymbol{Energy}$ plane.

2.6 Jost Function at a Resonance State

As explained in the Introduction, resonances are created when interacting particles are trapped together inside a potential barrier for a period of time $\boldsymbol{\tau}$. Quantum resonances are similar to bound states but are not stable as bound states. Resonances are also known as quasi-stationary or quasi-bound states. Spherically symmetric potential $\boldsymbol{V(r)}$ supporting resonances is the potential that describes for example, the decay of radioactive nuclei or of unstable particles [12]. Resonances have a finite lifetime and stochastically decay according to the radioactive law:

$$\boldsymbol{N = N_0 exp(-\Gamma t/\hbar)} \tag{15}$$

where,
$\boldsymbol{N_0}$ is an initial number of particles in an ensemble of quantum particles,
$\boldsymbol{N}$ is the number of particles in the ensemble at time $\boldsymbol{t}$,
$\boldsymbol{\Gamma}$ is the resonance width and is measured in units of energy. It is commonly known as the **decay rate**.

At resonance, the Hamiltonian has complex eigen values. In fact, the energy $\boldsymbol{E}$ has a negative imaginary part given as;

$$\boldsymbol{E = E_r + E_i} \quad \text{where} \quad \boldsymbol{E_i = -i\Gamma/2}$$

$$\text{then} \quad \boldsymbol{E_{resonance} = E_r - i\Gamma/2}$$

$$\text{and} \quad \boldsymbol{\Psi(\vec{r}, t) = \Psi(\vec{r}) e^{\frac{-i}{\hbar}(E_r - i\Gamma/2)t}}$$

The decay law of equation (15) is obtained, if we recall that the number of particles is determined by the probability density:

$$N \sim |\Psi|^2 \sim \exp(-\Gamma t/\hbar)$$

The half-life of the quantum resonance is given as

$$\tau_{1/2} = \frac{\hbar \ln 2}{\Gamma}$$

The bigger the value of Γ, the smaller the half-life and the faster the resonance decays. Bigger Γ hence, refers to more unstable resonance or shortlived resonance.

After a quasi-stationary state has been excited, the energy is distributed rapidly in all possible degrees of freedom. As it decays, the eigenfunction of Hamiltonian corresponding to the complex energies at resonance, consist of outgoing waves only. In relation to the radial wave function $u_\ell(E, r)$, it means that equation (12) consists of outgoing wave only. Therefore, similar to the case of a bound state, the wave function can then be expressed as:

$$u_\ell(E, r) \xrightarrow[r \to \infty]{} h_\ell^{(+)}(kr) f_\ell^{out}(E)$$

This implies that there is no incoming wave and the coefficient or amplitude $f_\ell^{(in)}(E)$ is zero.

Thus, the bound and resonant states are very similar and are both spectral points. They have similar boundary conditions. The difference is that the bound states have real negative energies while the resonances occur at complex energies.

Figure (4) schematically illustrates the trajectory of a quantum particle at a resonance. It forms a partially localised state which slowly leaks out. The particle then moves out of the localised state, randomly, without any reference to where it came from.

Owing to the fact that $f_\ell^{(in)}(E) = 0$ at resonances, the latter corresponds to spectral points on complex energy E plane and k plane. Figure (5) shows where the resonance states are located on the k plane and E plane.

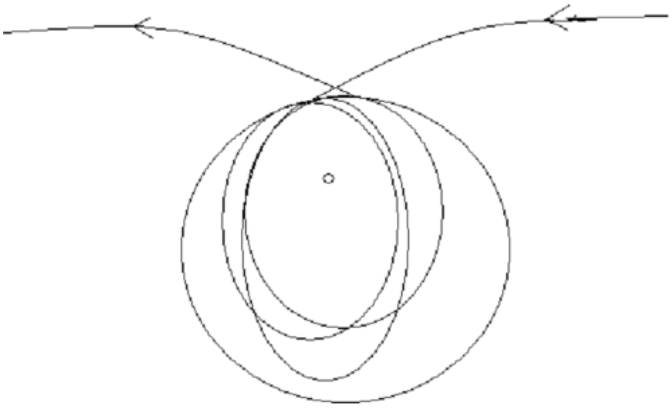

Figure 4: A resonance scattering orbit.

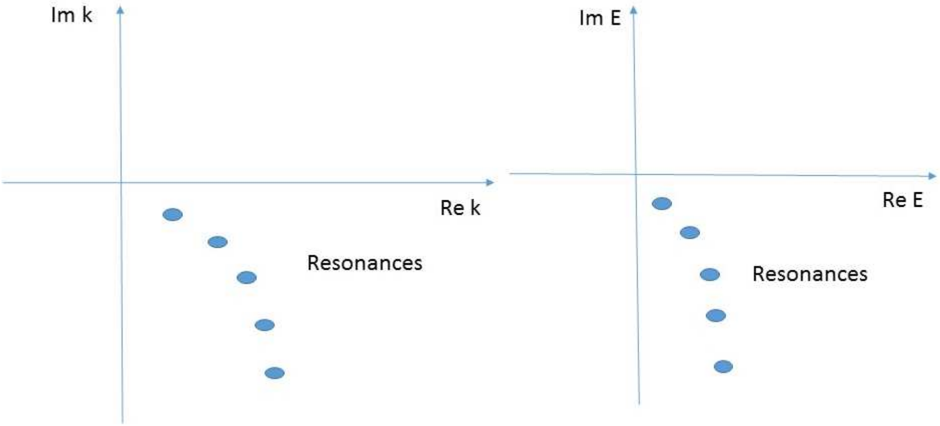

Figure 5: Resonances on the ***k*** plane and ***Energy*** plane.

2.7 Jost Function and the Scattering State

As seen in figure (6), transmission of a plane wave through a barrier and its reflection is in effect, a simplified scattering problem. In the world of atomic and sub-atomic particles, the only method to study the properties of these invisible objects is to collide them and watch what happens.

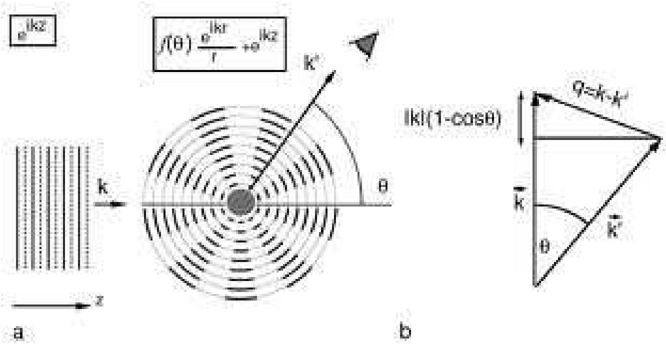

Figure 6: Differential cross-section of scattered wave $d\Omega$.

Suppose we have an incoming asymptotic state at $t = -\infty$, the transition from the initial to final state can be written as the action of an operator, called the S-matrix, whereby:

$$|\Psi >= \hat{S}|\Psi_{in} >$$

The energy E of scattering states is real and positive. The corresponding momentum k is thus real and positive. Applying the particle conservation principle to the incoming and outgoing waves, the flux of the particles is conserved. The absolute value of the amplitude of the incoming and outgoing waves should then be identical.

If the amplitude of incoming wave is equal to the amplitude of outgoing wave, then

$$|f_\ell^{(in)}(E)| = |f_\ell^{(out)}(E)| \quad \text{for} \quad E > 0$$

These amplitudes differ only by the phase factor.

The Riccati-Hankel solution is such that,

$$h_\ell^{(\pm)}(kr)]^* = h_\ell^{(\mp)}(kr) \quad \text{if} \quad Im(kr) = 0$$

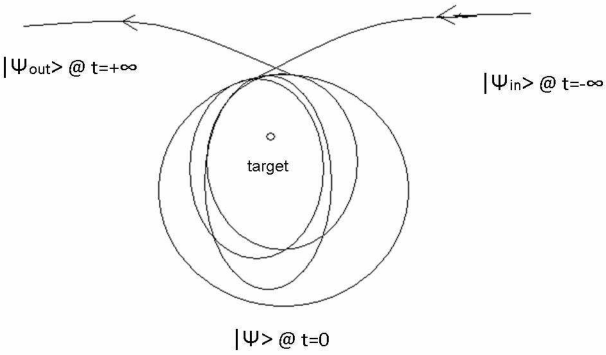

Figure 7: Transition between initial and final state

This leads to the fact that the amplitudes of the incoming and outgoing wave, which are essentially the Jost functions, should be complex conjugates of each other,

$$\boldsymbol{f_\ell^{(in)}(E) = [f_\ell^{(out)}(E)]^*} \quad \text{for} \quad \boldsymbol{E > 0}$$

Or we could write the amplitudes as:

$$\left\{ \begin{array}{l} \boldsymbol{f_\ell^{(in)}(E) = |f_\ell^{(in)}(E)| e^{-i\delta_\ell(E)}} \\ \boldsymbol{f_\ell^{(out)}(E) = |f_\ell^{(out)}(E)| e^{+i\delta_\ell(E)}} \end{array} \right. \quad \text{for} \quad \boldsymbol{E > 0} \tag{16}$$

The "real" function $\boldsymbol{\delta_\ell(E)}$ is called the *phase shift.*

From equation (16), it is clear that the incoming wave amplitude is transformed into the outgoing amplitude by a function $\boldsymbol{S_l(E)}$, such that,

$$\boldsymbol{f_\ell^{(out)}(E) = S_\ell(E) f^{(in)}(E)}$$

where,

$$\boldsymbol{S_\ell(E) = e^{i2\delta_\ell(E)}} \quad \text{for} \quad \boldsymbol{E > 0}$$

This transformation function $\boldsymbol{S_\ell(E)}$ is called the **S-matrix**. It contains the complete information about the scattering process. It can be expressed as the ratio of the incoming to the outgoing wave amplitude

$$S_\ell(E) = f_\ell^{(out)}(E)[f_\ell^{(in)}(E)]^{-1}$$

The S-matrix is analytic everywhere except for isolated poles. The poles are those points where the Jost function $f_\ell^{(in)}(E)$ is zero, that is, at the spectral points on the energy surface.

2.7.1 Relationship between Resonance and Scattering State

A resonance will show characteristically as a rapid rise of the scattering phase shift $\delta(E)$, and this surge corresponds to a time delay. Regarding the scattering of a wave packet, the delay is of the order [33]

$$\Delta t \sim \hbar \frac{\mathrm{d}\delta(E)}{\mathrm{d}E}$$

where,

$$\delta(E) = \delta_{bg}(E) + \delta_{res}(E)$$

and,

$$\delta_{res}(E) = \arctan\left(\frac{\Gamma/2}{E_r - E}\right) + n(E)\pi$$

for $\Gamma > 0$. The $n(E)$ is an integer depending on energy that may be optionally added to make $\delta_{res}(E)$ a continuous function of energy. Thus, the propagation of a wave packet in the presence of a resonance experiences a time delay of

$$\tau \sim \hbar\, \mathrm{d}\delta_{res}(E)/\,\mathrm{d}E$$

Using the first order approximation for the Jost function near a resonance spectral point where $E_0 = E_r - i\Gamma/2$ and the symmetry property, $f_\ell^{(out)} = f_\ell^{(in)*}$, which is valid for real positive energies, the S matrix on the real axis next to E_0 can be approximated to;

$$S_\ell(E) \approx \frac{f_\ell^{(in)*}(E)}{f_\ell^{(in)}(E)} \approx \frac{f_\ell^{(in)*}(E_0)(E - E_0)^*}{f_\ell^{(in)}(E_0)(E - E_0)} = e^{-2i\delta_\ell^{bg}} \frac{E - E_r - i\Gamma/2}{E - E_r + i\Gamma/2} \tag{17}$$

When the background phase shift $\delta_\ell^{bg} \approx 0$ then the resonance contributes to a partial wave cross section of;

$$\sigma_\ell^{res}(E) = \frac{4\pi}{k^2}(2L+1)\frac{\Gamma^2/4}{(E-E_r)^2+\Gamma^2/4} \tag{18}$$

Equation(18) is the Breit-Wigner resonance formula. It shows a clear peak at $E \approx E_r$ with a full width at half maximum of Γ [33] [35].

Using the $S_\ell-$ matrix as defined in (17), at resonance the function $S_\ell(E)$ will have a pole, where the denominator is zero, i.e, at $E_p = E_r - i\Gamma/2$. These are poles in the fourth quadrant of the complex energy plane close to and below the real energy axis. The existence of such a complex pole leads most theorists to *define* resonance by its pole position.

Mathematically, a resonance is therefore a pole of the S-matrix in the fourth complex energy quadrant with $Re(E_p) > 0$ and $Im(E_p) < 0$ where E_p is the energy at the resonance pole. Resonances may also be characterised as nearly-bound or almost-bound states. These are states that would be bound if the potential were stronger. In the complex plane, bound states are also poles on the negative real energy axis and on the positive imaginary $k-$ axis.

If the potential for a bound state becomes weaker, the pole moves towards zero energy (as shown in diagram below), and then it becomes a resonance if a potential barrier between large distances and the interior nuclear attraction.This trapping barrier could be the repulsive Coulomb barrier in the case of proton-nucleus scattering, or a centrifugal barrier for either neutrons or protons in angular momentum, $\ell > 0$ states [33]. The wide resonances are far away from the real axis. Wide resonances do not have a pronounced effect on scattering at real energies.

2.8 Spectral Points on the $k-$plane

The energy at which a bound state or a resonance occurs is the energy at which the incoming amplitude $f_\ell^{(in)}(E)$ is zero, i.e, the Jost function has a zero. By determining the zero of the Jost function, the bound state and resonance can be found on the energy plane.

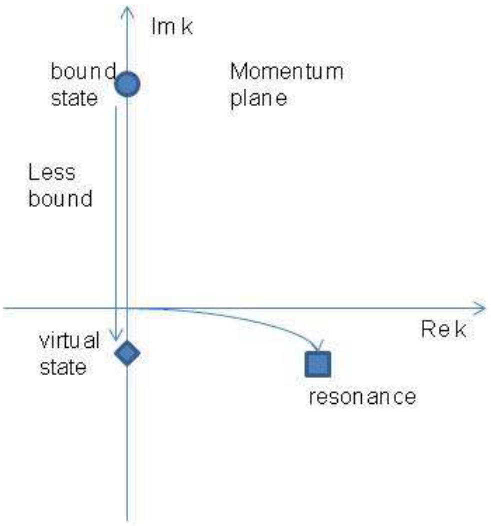

Figure 8: Trajectory of a bound state caused by a progressively weaker potential

Since

$$\boldsymbol{k^2 = \frac{2\mu}{\hbar^2}E} \qquad \text{then} \qquad \boldsymbol{E = \frac{\hbar^2}{2\mu}[(Rek)^2 - (Imk)^2 + i2(Rek)(Imk)]}$$

The spectral points can be plotted on the complex momentum $\boldsymbol{k}-$ plane as well. In this case,

1. The bound states are points on the positive imaginary $\boldsymbol{k}-$ axis,
2. The scattering states are along the positive real $\boldsymbol{k}-$ axis,
3. The resonance states are points in the fourth quadrant, between the real positive and the imaginary negative $\boldsymbol{k}-$ axes.

The figure below illustrates the plot of the spectral points on the complex $\boldsymbol{k}$ plane.

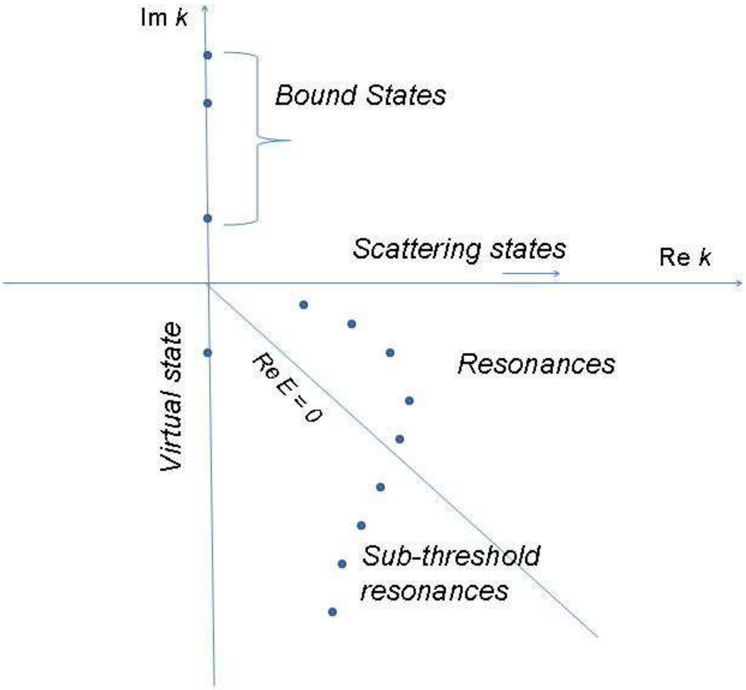

Figure 9: Spectral Points on $\boldsymbol{k}-$plane

3 Determination by Jost Method

The Jost function contains information about all spectral points. If this function can be calculated for any complex energy, then we would be able to locate the bound states and the resonances, using the fact that for these states,

$$f_\ell^{(in)}(E) = 0$$

In this section the Schrödinger equation is transformed in order to more easily determine the energy (or momentum k), at which spectral points occur, i.e, at which bound or resonance state occurs, by means of the Jost function.

Considering a quantum particle in a spherical potential $V(r)$, the radial Schrodinger equation is,

$$\left[\frac{d^2}{dr^2} + k^2 - \frac{\ell(\ell+1)}{r^2}\right] u_\ell(E,r) = V(r)u_\ell(E,r) \tag{19}$$

We recall that when the potential $V(r) = 0$, then the free radial Shrödinger equation is obtained:

$$\left[\frac{d^2}{dr^2} + k^2 - \frac{\ell(\ell+1)}{r^2}\right] u_\ell(E,r) = 0 \tag{20}$$

The solution to equation (20), as explained in previous chapter, is the Riccati-Bessel and Riccati-Neumann functions $j_\ell(kr)$ and $n_\ell(kr)$ or the Riccati-Hankel functions $h_\ell^{(\pm)}(kr)$. To simplify the notation, the incoming and outgoinf spherical waves can be denoted as:

$$W_\ell^{(in)}(E,r) = h_\ell^{(-)}(kr) \tag{21}$$

$$W_\ell^{(out)}(E,r) = h_\ell^{(+)}(kr) \tag{22}$$

Hence the general solution to (20) is a linear combination:

$$W_\ell^{(in)} F_\ell^{(in)} + W_\ell^{(out)} F_\ell^{(out)}$$

where $\boldsymbol{F_\ell^{(in/out)}}$ are some constant parameters.

The solution to the equation (19) where the potential is non-zero can be expressed similarly:

$$\boldsymbol{u_\ell(E,r) = W_\ell^{(in)}(E,r)F_\ell^{(in)}(E,r) + W_\ell^{(out)}(E,r)F_\ell^{(out)}(E,r)} \tag{23}$$

where $\boldsymbol{F_\ell^{(in/out)}(E,r)}$ are unknown functions.

The variation parameters method from the theory of linear differential equation can be used to solve the equation.

It must be noted that $\boldsymbol{F_\ell^{(in/out)}(E,r)}$ are unknown functions introduced to solve the unknown function $\boldsymbol{u_\ell(E,r)}$. As such these three unknowns must be related to each other and cannot be independent of one another. An arbitrary condition can be imposed that relates the unknown functions as follows:

$$\boldsymbol{W_\ell^{(in)}(E,r)\partial_r F_\ell^{(in)}(E,r) + W_\ell^{(out)}(E,r)\partial_r F_\ell^{(out)}(E,r) = 0} \tag{24}$$

This condition is known as the Lagrange Condition and is well-defined in calculus [36].

Using the lagrange condition (24), the second derivative of $\boldsymbol{u_\ell(E,r)}$ is:

$$\boldsymbol{\frac{\mathrm{d}^2}{\mathrm{d}r^2}u_\ell = W_\ell^{\prime\prime(in)}F_\ell^{(in)} + W_\ell^{\prime\prime(out)}F_\ell^{(out)} + W_\ell^{\prime(in)}F_\ell^{\prime(in)} + W_\ell^{\prime(out)}F_\ell^{\prime(out)}}$$

When substituting (23) into (19), the following is obtained:

$$\boldsymbol{\left\{\left[\frac{\mathrm{d}^2}{\mathrm{d}r^2} + k^2 - \frac{\ell(\ell+1)}{r^2}\right]W_\ell^{(in)}(E,r)\right\}F_\ell^{(in)}(E,r)} \tag{25}$$

$$\boldsymbol{+\left\{\left[\frac{\mathrm{d}^2}{\mathrm{d}r^2} + k^2 - \frac{\ell(\ell+1)}{r^2}\right]W_\ell^{(out)}(E,r)\right\}F_\ell^{(out)}(E,r)} \tag{26}$$

$$\boldsymbol{+W_\ell^{\prime(in)}(E,r)F_\ell^{\prime(in)}(E,r) + W_\ell^{\prime(out)}(E,r)F_\ell^{\prime(out)}(E,r) = V(r)u_\ell(E,r)} \quad , \tag{27}$$

The first two terms in the curly brackets disappear since $\boldsymbol{W_\ell^{(in)}(E,r)}$ and $\boldsymbol{W_\ell^{(out)}(E,r)}$ are solutions to (20). Therefore we get:

$$\boldsymbol{W_\ell'^{(in)} F_\ell'^{(in)} + W_\ell'^{(out)} F_\ell'^{(out)} = V \left[W_\ell^{(in)} F_\ell^{(in)} + W_\ell^{(out)} F_\ell^{(out)} \right]} \tag{28}$$

From equation (24), it follows that:

$$\boldsymbol{F_\ell'^{(out)} = -\left[W_\ell^{(out)} \right]^{-1} W_\ell^{(in)} F_\ell'^{(in)}} \tag{29}$$

Substituting (29) into (28) results into:

$$\boldsymbol{\left[W_\ell^{(out)} \right]^{-1} W_\ell^{(out)} \left\{ W_\ell'^{(in)} - W_\ell'^{(out)} \left[W_\ell^{(out)} \right]^{-1} W_\ell^{(in)} \right\} F_\ell'^{(in)}}$$
$$\boldsymbol{= V \left[W_\ell^{(in)} F_\ell^{(in)} + W_\ell^{(out)} F_\ell^{(out)} \right]}$$

And then,

$$\boldsymbol{F_\ell'^{(in)} = \left[W_\ell^{(out)} W_\ell'^{(in)} - W_\ell'^{(out)} W_\ell^{(in)} \right]^{-1} W_\ell^{(out)} V \left[W_\ell^{(in)} F_\ell^{(in)} + W_\ell^{(out)} F_\ell^{(out)} \right]} \tag{30}$$

Applying the same condition as (29) to $\boldsymbol{F_\ell'^{(in)}}$ results into:

$$\boldsymbol{F_\ell'^{(out)} = \left[W_\ell^{(in)} W_\ell'^{(out)} - W_\ell'^{(in)} W_\ell^{(out)} \right]^{-1} W_\ell^{(in)} V \left[W_\ell^{(in)} F_\ell^{(in)} + W_\ell^{(out)} F_\ell^{(out)} \right]} \tag{31}$$

The first factors of (50) and (51) differ only by the sign and are equal to the inverted Wronskian of the incoming and the outgoing spherical waves, i.e, the Riccati-Hankel functions,

$$\boldsymbol{h_\ell^{(-)}(kr)\partial_r h_\ell^{(+)}(kr) - h_\ell^{(+)}(kr)\partial_r h_\ell^{(-)}(kr) = 2ik} \tag{32}$$

Thus finally the second order differential Shrödinger equation (19) is reduced to a coupled system of the first order differential equations of the Jost functions;

$$\boldsymbol{\begin{cases} \partial_r F_\ell^{(in)}(E,r) = -\frac{h_\ell^{(+)}(kr)}{2ik} V(r) \left[h_\ell^{(-)}(kr) F_\ell^{(in)}(E,r) + h_\ell^{(+)}(kr) F_\ell^{(out)}(E,r) \right] \\ \partial_r F_\ell^{(out)}(E,r) = \frac{h_\ell^{(-)}(kr)}{2ik} V(r) \left[h_\ell^{(-)}(kr) F_\ell^{(in)}(E,r) + h_\ell^{(+)}(kr) F_\ell^{(out)}(E,r) \right] \end{cases}} \tag{33}$$

The system of equation (33) is completely equivalent to the Schrödinger equation (19), from which we started. It is however more convenient for locating the spectral points.

Indeed, since $\boldsymbol{V(r)} \underset{r\to\infty}{\longrightarrow} \boldsymbol{0}$ the right hand sides of equation(33) at large distances vanish, which means that $\boldsymbol{F_\ell^{(in/out)}(E,r)}$ become constant. These constants are the Jost functions. In other words, these equations give us a simple way of direct calculation of the Jost functions [37].

3.1 Boundary Conditions for $F_\ell^{(in/out)}(E,r)$

In order to solve (33), the boundary conditions on $F_\ell^{(in/out)}(E,r)$ have to be established.

Recalling that the radial wave function should vanish at the centre, that is, $u_\ell(E,0)=0$, and given the general expression for $u_\ell(E,r)$ as;

$$u_\ell(E,r)=h_\ell^{(-)}(kr)F_\ell^{(in)}(E,r)+h_\ell^{(+)}(kr)F_\ell^{(out)}(E,r)$$

(referring to equation (23), it implies that the two functions $F_\ell^{(in/out)}(E,r)$ should be equal to the same constant, when $r\to 0$.

It is only when the two functions $F_\ell^{(in/out)}(E,r)$ are equal that $u_\ell(E,0)=0$, because,

$$h_\ell^{(+)}(kr)+h_\ell^{(-)}(kr)=2j_\ell(kr)\underset{r\to 0}{\longrightarrow}0$$

A simple boundary condition could then be;

$$F_\ell^{(in/out)}(E,0)=1 \tag{34}$$

Since (33) are of the first order, the boundary conditions (34) imposed at $r=0$, completely determine the solutions as well as the wave function of (23).

In the case of $r\to\infty$, and the potential tends to vanish, the radial wave function (23) can be written as:

$$u_\ell(E,r)\underset{r\to\infty}{\longrightarrow}h_\ell^{(-)}(kr)f_\ell^{(in)}(E)+h_\ell^{(+)}(kr)f_\ell^{(out)}(E) \tag{35}$$

Then the Jost functions are the limits as $r\to\infty$:

$$f_\ell^{(in)}(E)=\lim_{r\to\infty}F_\ell^{(in)}(E,r) \tag{36}$$

and

$$f_\ell^{(out)}(E)=\lim_{r\to\infty}F_\ell^{(out)}(E,r) \tag{37}$$

Under the assumption that $V(r)=0$ at distances greater than R, the limit of the above equations is reached at $r=R$, because beyond this point the right hand sides of equations (33) are zero and therefore the $F_\ell^{(in/out)}(E,r)$ are constants since their first derivatives vanish. This means that $F_\ell^{(in/out)}(E,r)$ are the Jost functions for the potential that cuts off abruptly at the point r.

The differential equations of (33) determining the functions $F_\ell^{(in/out)}(E,r)$ can be written simply as;

$$\partial_r F_\ell^{(in)}(E,r) = -\frac{h_\ell^{(+)}(kr)}{2ik} V(r) u_\ell(E,r) \tag{38}$$

$$\partial_r F_\ell^{(out)}(E,r) = \frac{h_\ell^{(-)}(kr)}{2ik} V(r) u_\ell(E,r) \tag{39}$$

If the first derivative of the Jost function do not vanish as $r \to \infty$ i.e., if the following conditions are not satisfied;

$$\partial_r F_\ell^{(in/out)} \to 0 \quad \text{as} \quad r \to \infty$$

then,

$$F_\ell^{(in/out)} \not\to \text{constant} \quad r \to \infty$$

That is, $F_\ell^{(in/out)}$ cannot have finite limits, and hence diverge.

Furthermore for these limits to exist, the first order derivatives must decrease to 0, faster than $\sim r^{-1}$. This is possible in the case of short range potentials that vanish faster at infinity than the Coulomb potential (i.e.,$-e^2/r$).

Assuming that

$$V(r) \propto \frac{1}{r^{1+\epsilon}} \quad \text{where} \quad \epsilon > 0$$

then from (38) and (39), we can further assume that

$$\partial_r F_\ell^{(in/out)}(E,r) \propto \frac{1}{r^{1+\epsilon}}$$

This implies that the integral will be;

$$F_\ell^{(in/out)}(E,r) \underset{r\to\infty}{\sim} \int \frac{dr}{r^{1+\epsilon}} = \left(\text{const} \quad - \frac{1}{\epsilon r^{\epsilon}}\right) \underset{r\to\infty}{\to} \text{const}$$

At large distances the Riccati-Hankel functions, independently of the value of the angular momentum ℓ, behave exponentially [27];

$$h_\ell^{(\pm)}(kr) \underset{r\to\infty}{\longrightarrow} \mp iexp[\pm i(kr - \ell\pi/2)]$$

and, since:

$$\exp{(\mp i\ell\pi/2)} = \exp{(i\pi/2)(\mp\ell)} = i^{\mp\ell}$$

then,

$$h_\ell(kr) \underset{|kr|\to\infty}{\longrightarrow} (\mp i)^{\ell+1}\exp{(\pm ikr)}$$

Given that;

$$u_\ell(E,r) \underset{r\to\infty}{\longrightarrow} h_\ell^{(-)}(kr)f_\ell^{(in)}(E) + h_\ell^{(+)}(kr)f_\ell^{(out)}(E)$$

By substituting the asymptotes of the Riccati-Hankel functions in the above equation, we can rewrite the above equation as;

$$u_\ell(E,r) \underset{r\to\infty}{\longrightarrow} a_\ell(E)\exp{(-ikr)} + b_\ell(E)\exp{(+ikr)} \qquad (40)$$

Equation (40) is in effect the asymptotic behavior (as $r \to \infty$) of the radial wave function $u_\ell(E,r)$ on the momentum k-plane.

The coefficients $a_\ell(E)$ and $b_\ell(E)$ are related to the Jost functions at large distances, i.e,

$$a_\ell(E) = (i)^{\ell+1}f_\ell^{(in)}(E) \quad \text{and} \quad b_\ell(E) = (-i)^{\ell+1}f_\ell^{(out)}(E)$$

It is important to note that $a_\ell(E)$ and $b_\ell(E)$ are r-independent functions of the energy only.

By substituting equation (40) into (38) and (39), the following are obtained;

$$\partial_r F_\ell^{(in)}(E,r) \underset{r\to\infty}{\longrightarrow} \frac{(-i)^\ell}{2k}V(r)\left[a_\ell(E) + b_\ell(E)e^{(2ikr)}\right] \qquad (41)$$

and

$$\partial_r F_\ell^{(out)}(E,r) \underset{r\to\infty}{\longrightarrow} \frac{(i)^\ell}{2k}V(r)\left[a_\ell(E)e^{(-2ikr)} + b_\ell(E)\right] \qquad (42)$$

Using the asymptotic behaviour of the first order partial derivative of the Jost functions (as outlined above), the behavior of the Jost functions $F_\ell^{(in/out)}(E,r)$, as $r \to \infty$, for different values of k, can be analysed on the complex k-plane.

3.2 Asymptotics on the k-plane

Let us consider various domains of the k-plane.

The momentum k is real

In this case, both derivatives $\partial_r F_\ell^{(in/out)}$ vanish fast enough, because we assumed that the potential vanishes faster than the Coulomb potential ($\propto 1/r$). It implies that when k is real, both Jost functions $F_\ell^{(in/out)}$ converge to a constant.

The momentum k has a positive imaginary part, but is not a spectral point

Since k does not coincide with a spectral point k_n, both $a_\ell(E)$ and $b_\ell(E)$ are nonzero. The factors $e^{-2Im(kr)}$ and $e^{+2Im(kr)}$ on the right hand sides of these equations, play the dominant roles. As $r \to \infty$, $\partial_r F_\ell^{(in)} \to 0$. Hence, the function $F_\ell^{(in)}(E, r)$ converges to a constant, while $F_\ell^{(out)}(E, r)$ diverges.

The momentum k has a negative imaginary part, but is not a spectral point

As is easily seen, the situation is just opposite to the one in the previous item, i.e., the function $F_\ell^{(out)}(E, r)$ converges while $F_\ell^{(in)}(E, r)$ diverges.

The momentum $k = k_n$ is a spectral point

By definition of spectral points (refer to the first two chapters), $a_\ell(E_n) = 0$, the incoming wave is zero and hence only the outgoing amplitude i.e, $F_\ell^{(out)}(E, r)$ converges irrespective of the sign of Imk_n.

Referring to equation (41), $F_\ell^{(in)}(E_n, r)$ converges to its limiting value only if Im$k_n > 0$.

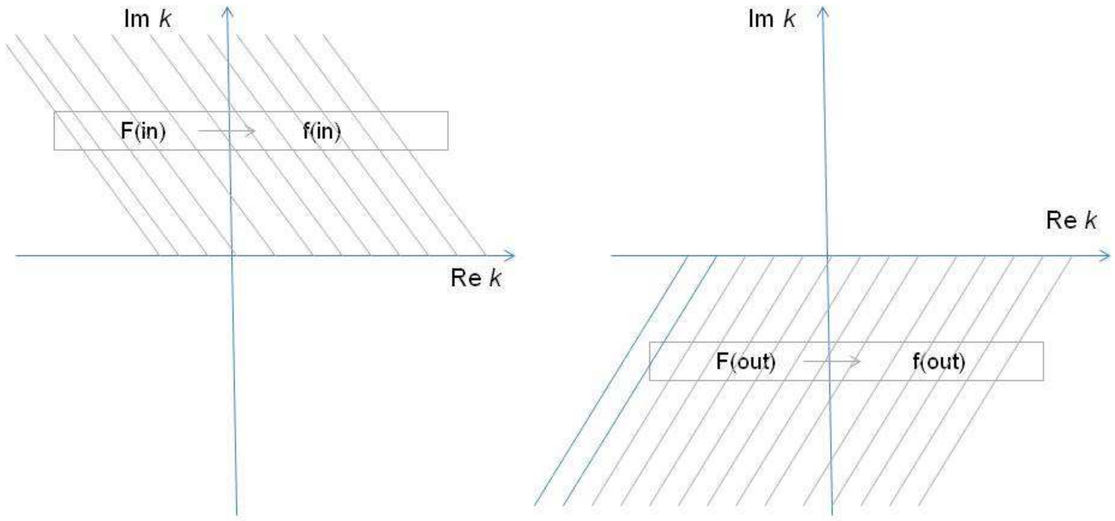

Figure 10: Domains of the k-plane where the functions $F_l^{(in/out)}(E,r)$ have finite limits

Summary of the domains where the limits of $F_\ell^{(in/out)}(E,r)$ exist

The line $Im(kr) = 0$ divides the k-plane in two domains. The upper domain is the domain where $Im(kr)$ is positive and ≥ 0. The lower domain is where $Im(kr)$ is negative or $Im(kr) \leq 0$. The function $F_l^{(in)}(E,r)$ converges to its limiting value $f_l^{(in)}(E)$ as $r \to \infty$, if $Im(kr) \geq 0$. The function $F_l^{(out)}(E,r)$ converges to $f_l^{(out)}(E)$ if $Im(kr) \leq 0$ at large r. At all spectral points $k = k_n$ irrespective of the sign of $Im(kr)$.

$$F_l^{(in)}(E,r) \underset{r\to\infty}{\longrightarrow} f_l^{(in)}(E) \qquad \text{if} \quad Im(kr) \geq 0 \tag{43}$$

$$F_l^{(out)}(E,r) \underset{r\to\infty}{\longrightarrow} f_l^{(out)}(E) \qquad \text{if} \quad Im(kr) \leq 0 \tag{44}$$

$$F_l^{(out)}(E_n,r) \underset{r\to\infty}{\longrightarrow} f_l^{(out)}(E_n) \qquad \text{at all spectral points} \quad E_n \tag{45}$$

3.3 Complex Scaling Method

We have so far determined the Jost functions $\boldsymbol{F_\ell^{(in/out)}(E,r)}$, assuming that the potential is cut off at $\boldsymbol{r = R}$. The solution is flawed however, when the potential extends to infinity. The problem is that in certain domains of the E-surface, the limiting values of $\boldsymbol{f_\ell^{(in/out)}(E)}$ cannot be reached, by integrating the coupled differential equations (33) along the real r-axis.

To circumvent this problem that occurs as we move away from the real $\boldsymbol{E}$-axis, the independent variable $\boldsymbol{r}$ in the Schrödinger equation can be considered as a complex variable. This is acceptable since the energy and the angular momentum are complex and the problem arises at complex values of $\boldsymbol{E}$.

It can also be proven that a solution $\boldsymbol{\varphi(z)}$ of the differential equation;

$$\boldsymbol{\frac{d^2\varphi(z)}{dz^2} + J(z)\varphi(z) = 0}$$

is an analytic function of $\boldsymbol{z}$ everywhere in the domain of analyticity of $\boldsymbol{J(z)}$. Therefore, if the potential $\boldsymbol{V(r)}$ is an analytic function, then the wave function $\boldsymbol{u_\ell(E,r)}$ is also an analytic function of $\boldsymbol{r}$. Thus, if we want to calculate $\boldsymbol{u_\ell(E,r)}$ at a point $\boldsymbol{R}$ on the real axis, the Schrödinger equation can be integrated from $\boldsymbol{r = 0}$ to $\boldsymbol{r = R}$ either directly along the real axis or moving into the complex plane of $\boldsymbol{r}$.

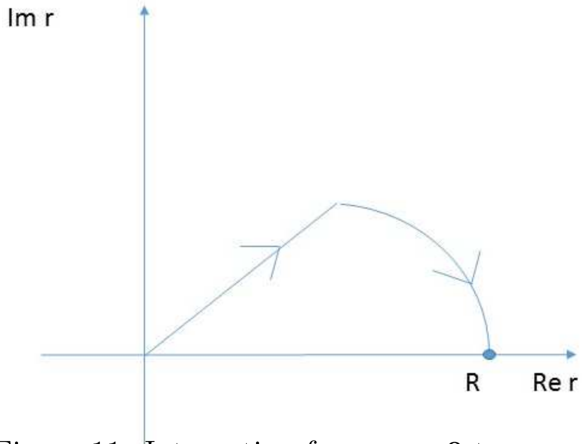

Figure 11: Integration from $\boldsymbol{r = 0}$ to $\boldsymbol{r = R}$

We can thus calculate the Jost functions using the definition of a complex $\boldsymbol{r}$ as,

$$\boldsymbol{r} = \boldsymbol{\rho e^{i\theta}} \qquad , \qquad \boldsymbol{\rho} = |\boldsymbol{r}| \tag{46}$$

The acceptable range for the rotation angle $\boldsymbol{\theta}$ is limited by the interval

$$-\pi/2 < \theta < +\pi/2 \tag{47}$$

Outside of this interval the incoming and outgoing waves ($\sim \boldsymbol{e^{\mp ikr}}$) swap roles. This interval can be narrowed further through the properties of the function $\boldsymbol{V(r)}$. The angle should be such that the potential vanishes at the far end of the ray (46) faster than $\boldsymbol{1/|r|}$,

$$\int_{|R'|}^{\infty} |V(\rho e^{i\theta})| d\rho < \infty \tag{48}$$

otherwise, the functions $\boldsymbol{F_\ell^{(in/out)}(E, r)}$ do not converge to constant values.

On the ray (46), the coupled first order differential equations of the incoming and outgoing Jost functions become;

$$\begin{cases} \partial_\rho F_\ell^{(in)}(E, \rho, \theta) = -\frac{e^{i\theta} h_\ell^{(+)}(k\rho)}{2ik} V(r) \times \\ \left[h_\ell^{(-)}(k\rho) F_\ell^{(in)}(E, \rho) + h_\ell^{(+)}(k\rho) F_\ell^{(out)}(E, \rho) \right] \\ \partial_\rho F_\ell^{(out)}(E, \rho, \theta) = \frac{e^{i\theta} h_\ell^{(-)}(k\rho)}{2ik} V(\rho) \times \\ \left[h_\ell^{(-)}(k\rho) F_\ell^{(in)}(E, \rho) + h_\ell^{(+)}(k\rho) F_\ell^{(out)}(E, \rho) \right] \end{cases} \tag{49}$$

where the derivatives are with respect to the real variable $\boldsymbol{\rho}$ and not $\boldsymbol{r}$. The boundary conditions for these equations remain the same as in equation (33).

To derive the conditions for the convergence of the limits, instead of the real $\boldsymbol{k}$-axis (Im$\boldsymbol{k}$=0), on which both limits exist, we use the line Im($\boldsymbol{kr}$)= $\boldsymbol{\rho}$Im($\boldsymbol{ke^{i\theta}}$)=0. Based on condition (48), we obtain

$$F_l^{(in)}(E, \rho e^{i\theta}) \underset{\rho\to\infty}{\longrightarrow} f_l^{(in)}(E) \qquad \text{if} \qquad Im(ke^{i\theta}) \geq 0 \tag{50}$$

$$F_l^{(out)}(E, \rho e^{i\theta}) \underset{\rho\to\infty}{\longrightarrow} f_l^{(out)}(E) \qquad \text{if} \qquad Im(ke^{i\theta}) \leq 0 \tag{51}$$

$$\boldsymbol{F_l^{(out)}(E_n, \rho e^{i\theta}) \underset{\rho\to\infty}{\rightarrow} f_l^{(out)}(E_n)} \quad \text{at all spectral points} \quad \boldsymbol{E_n} \tag{52}$$

When $\boldsymbol{r}$ is real, the sign of $\boldsymbol{Im(kr)}$ depends purely on the sign of $\boldsymbol{Im(k)}$. In the case of complex rotation, an appropriate rotation angle $\boldsymbol{\theta}$ can be chosen such that $\boldsymbol{Im(ke^{i\theta})}$ is either positive or negative. Figures (12) and (13) below illustrate the domain where the functions $\boldsymbol{F_\ell^{(in/out)}(E, r)}$ converge, ie., have finite limits on the $\boldsymbol{k}$-plane, based on angle $\boldsymbol{\theta}$ [37].

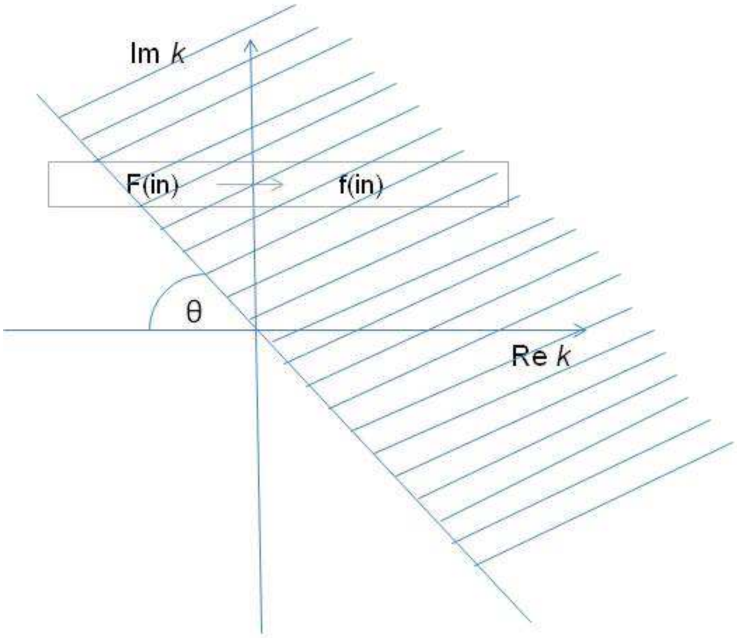

Figure 12: Complex Scaling position of function $\boldsymbol{F_l^{(in)}(E, r)}$

Since the energy is a quadratic function of the momentum $\boldsymbol{k}$, that is,

$$\boldsymbol{E = \hbar^2 k^2/(2\mu)}$$

the effect of the complex rotation in the complex energy plane is the following:

- the discrete bound state spectrum which lies on the negative energy axis remains unchanged;

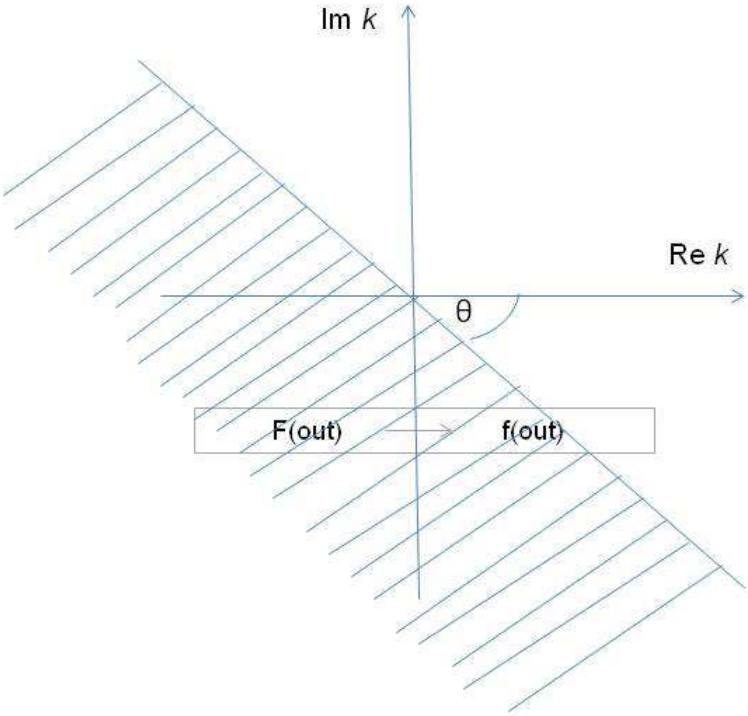

Figure 13: Complex Scaling position of function $\boldsymbol{F_l^{(out)}(E,r)}$

- the branch cut (the discontinuity) along the real positive energy axis rotates clockwise by the angle $\boldsymbol{2\theta}$;
- resonances in the lower half of the complex energy plane located in the sector which is bounded by the new rotated cut line and the positive energy axis get exposed and become isolated [15].

By considering complex values of $\boldsymbol{r}$, the function $\boldsymbol{f_\ell^{(in/out)}(E)}$ is made analytically continuous across the dividing line to the domains where the equations (33) do not give finite values of these functions, that is, when $\boldsymbol{V(r)}$ extends to infinity.

Hence complex rotation solves the problem of calculating the Jost function $\boldsymbol{f_\ell^{(in)}(E)}$ in the fourth quadrant of the $\boldsymbol{k}$-plane. An appropriate positive angle $\boldsymbol{\theta}$ can be chosen which turns the dividing line and thus allows access to the resonance domain. Resonance spectral points can then be calculated. The rotation is illustrated in the diagram (14) below. The complex rotation method is also commonly called the complex scaling method, owing to the

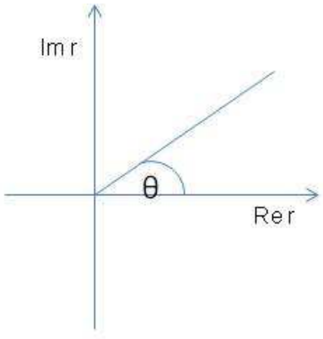

Figure 14: Appropriate angle $\boldsymbol{\theta}$ for rotation

fact that the coordinate $\boldsymbol{r}$ is being scaled by the factor $\mathbf{exp}\,(\boldsymbol{i\theta})$, within the limits of angle $\boldsymbol{\theta}$.

Complex scaling may be viewed as a technique which "compresses" information about the evolution of a resonance state at infinity into a small well-defined space. The tail in spatial domain of a single, time independent, square integrable resonance wave function contains all the information about the quantum system, including information on partial width and the way in which the system evolves as the separation between the quantum particle and the 'target' increases to infinity $\boldsymbol{\infty}$.

The parameter $\boldsymbol{\Gamma}$ which is the imaginary part of the complex resonance energy, is associated with the rate of decay and with the inverse lifetime of the 'particle-target' system. The angle $\boldsymbol{\theta}$ can be interpreted as a control parameter which brings information of the decay process from $\boldsymbol{\infty}$ to a finite region in space, the size of which depends on the value of $\boldsymbol{\theta}$. As $\boldsymbol{\theta}$ increases, the information about the decay process is compressed into a smaller part of the coordinate space. However, $\boldsymbol{\theta}$ cannot exceed a critical value, as defined in (47) [12].

Figures (15) and (16) illustrate the rotation on the $\boldsymbol{k}$- plane and $\boldsymbol{E}$- plane respectively.

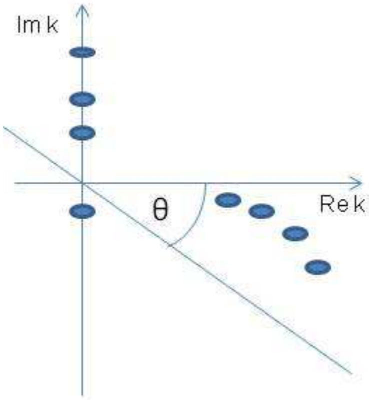

Figure 15: Complex Rotation in the $\boldsymbol{k}$-plane

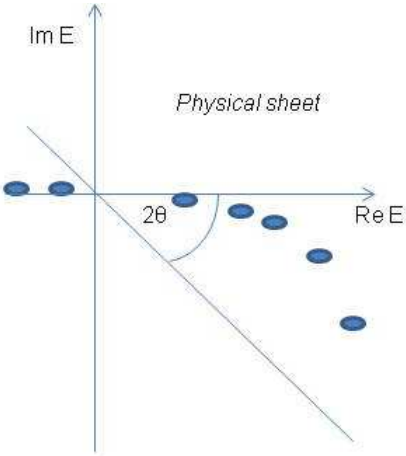

Figure 16: Result in the $\boldsymbol{E}$-plane

4 Numerical Calculation

Considering a single non-relativistic particle at a distance r from the centre, under a spherical potential $V(r)$, in order to determine the location of the resonances, a direct method of finding the spectral points on the complex-k plane is applied.

As explained in the previous section, the second order differential Schrödinger equation can be transformed into a coupled system of partial first order differential equations of the incoming and outgoing Jost function $F_\ell^{(in/out)}(E, r)$.

In order to circumvent the problem of potential that tails off to infinity very slowly, the complex scaling method is used, such that

$$r = \rho \exp^{i\theta} \quad \text{where} \quad -\pi/2, \theta < +\pi/2$$

At the centre of the sphere, the boundary condition is:

$$F_\ell^{(in/out)}(E, 0) = 1 \quad \text{at} \quad r = 0$$

As $r \rightarrow \infty$, the limit of the Jost function is defined as:

$$\lim_{r\rightarrow\infty} F_\ell^{(in/out)}(E, r) = f_\ell^{(in/out)}(E)$$

The procedure for calculating the Jost function is based on solving the couple first order partial differential equation from $\rho = 0$ to some maximum ρ where $F_\ell^{(in/out)}$ reaches a constant value or converges.

The spectral points corresponding to resonance states can be found in the complex k domain by taking the rotation angle θ over a large enough region. The zero of the Jost function is then determined in that region of the k domain.

Then, the partial differential equations are solved through an iterative integration approach, namely the Newton method. A computational program in Fortran, attached in Annexure A, is used to simulate the Newton numerical method.

4.1 The Complex Absorbing Potential

When a particle collides with a target, the collision is not always purely elastic. For example, if electrons are incident on hydrogen atoms in the ground state, and if these electrons have a kinetic energy larger than the excitation energy of the $\boldsymbol{n = 2}$ hydrogen state (10.2eV), then electron impact excitation of $\boldsymbol{n = 2}$ states, which are inelastic collisions, will occur in addition to elastic scattering. The fact that "non-elastic" processes take place means that some particles have been removed from the incident (elastic) channel, or in other words have been "absorbed".

This absorption of particles can be represented mathematically by introducing a complex or "optical" potential having a negative imaginary part. To prove this, let us start with the Schrödinger equation;

$$i\hbar\frac{\partial\psi}{\partial t} = -\frac{\hbar^2}{2\mu}\nabla^2\psi + V\psi \tag{53}$$

and its complex conjugate;

$$i\hbar\frac{\partial\psi^*}{\partial t} = -\frac{\hbar^2}{2\mu}\nabla^2\psi^* + V^*\psi^* \tag{54}$$

where $V \neq V^*$. Indeed, let the potential be complex as in;

$$V(r) = V_R(r) + iV_I(r) \tag{55}$$

If we multiply (53) by ψ^* and (54) by ψ, and we subtract the two equations, then we obtain

$$i\hbar\frac{\partial(\psi^*\psi)}{\partial t} = -\frac{\hbar^2}{2\mu}\nabla\cdot[\psi^*\nabla\psi - (\nabla\psi^*)\psi] + (V - V^*)\psi^*\psi \tag{56}$$

The probability density is given as;

$$\rho = \psi\psi^*$$

and the probability current density is;

$$\vec{j} = \tfrac{\hbar}{2\mu i}[\psi^*\nabla\psi - (\nabla\psi^*)\psi]$$

Thus, equation (56) can be rewritten in the form of the continuity equation, viz.

$$\frac{\partial \rho}{\partial t} + \nabla \cdot \vec{j} = \frac{1}{i\hbar}(V - V^*)\rho \tag{57}$$

If the potential is real, the right side of equation (57) is zero, and therefore any change of ρ at a point $\vec{r}$ is exactly compensated by the flux $\nabla \cdot \vec{j}$ of probability through a surface enclosing this point. If the potential is complex, this is not so because,

$$\frac{\partial \rho}{\partial t} + \nabla \cdot \vec{j} = \frac{2\rho}{\hbar} V_I \tag{58}$$

Thus equation (58) shows that if $V_I > 0$ an increase of ρ exceeds the incoming flux, which means the presence of a source. If $V_I < 0$ an increase of ρ is less than the flux, which means the presence of a sink. A sink also means there is local absorption of the incident beam. The rate of absorption of the incident particles per second per unit volume at the point r is $2|V_I|$. Thus when the complex potential has a negative imaginary part, absorption occurs during the scattering process [19] [33].

The main effect of the imaginary part of the potential is to lessen the scattering intensity. Complex potentials including of imaginary component, can be used to study elastic scattering between composite systems (e.g., ions, atoms and molecules) [20] [21].

4.2 Resonance Observation

In this numerical calculation, the objective is to study what happens to the spectral points when the potential acquires an imaginary part. The complex potential used is:

$$V(r) = 7.5r^2 \exp(-r) - i\alpha \exp(-r)$$

where

$$V_R = 7.5r^2 \exp(-r) \qquad V_I = -\alpha \exp(-r)$$

The figure (17) that follows is the real component of the complex potential used in this thesis. The main reason for using this potential is that it has been successfully applied in other similar numerical experiments. The results are therefore well established and predictable.

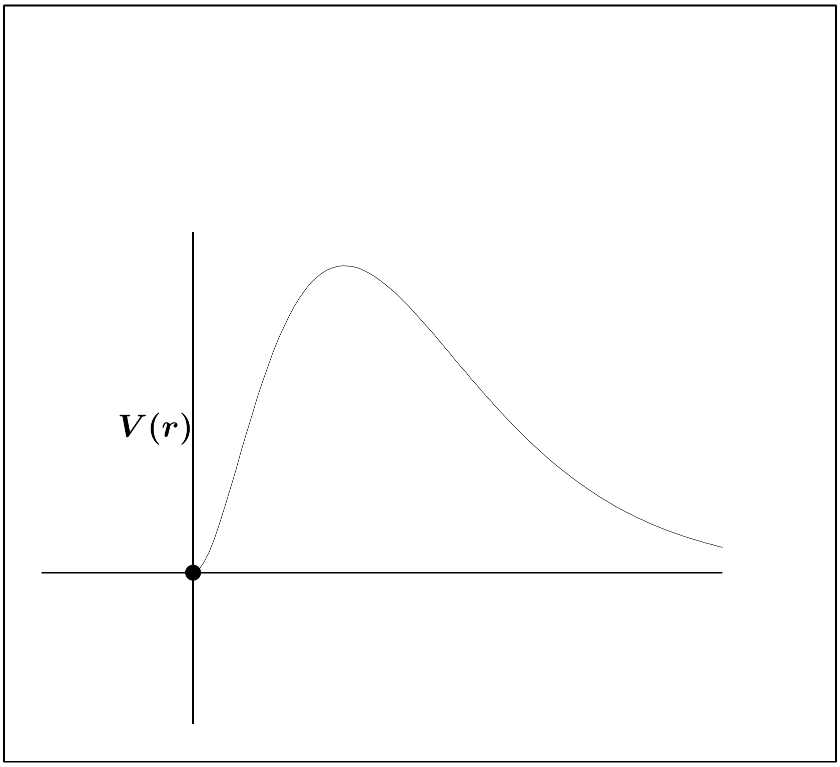

Figure 17: Plot of Potential used in our computation

When an imaginary component is added, the computational program is run for values of α from 0 to 0.01 incrementing by 0.001. For each value of

$\boldsymbol{\alpha}$, the zeroes of the Jost function is calculated. The following table (1) presents the values of real and imaginary momentum that were entered into the computational program, and the resulting real and imaginary momentum $\boldsymbol{k}$ where the zeroes of the Jost function occur, i.e, the location of resonances. These resonances were thus located as the imaginary potential became more negative.

Imaginary potential	Input momentum		Resonant momentum	
$\boldsymbol{\alpha}$ of $\boldsymbol{V_I}$	Inp Re(k)	Inp Im(k)	Res Re(k)	Res Im(k)
$\boldsymbol{0.0 \leqslant \alpha \leqslant 0.02}$	2.6	0	2.6175529443	-0.0090360903
	3	1	3.012653958	-0.3991257473
	3	1.5	3.0218703414	-1.65695133712
	2.3	1.8	3.036237501	-1.0352490003

Table 1: Corresponding resonant momentum for values of component of $\boldsymbol{V_I}$ between $\boldsymbol{0.0 \leq \alpha \leq 0.02}$

The resulting momentum values $\boldsymbol{k}$ where the zeroes of the Jost function occur, are plotted on the complex $\boldsymbol{k}$ plane. Figure (18) shows that the zeroes occur for values of the momentum located in the fourth quadrant. This complies with the theory that spectal points corresponding to resonance states, are found in the fourth quadrant of the complex $\boldsymbol{k}$ plane, where the $\boldsymbol{Re(k)}$ is positive and the $\boldsymbol{Im(k)}$ is negative.

The plot further shows that the resonant zeroes follow a downward path. The resonance spectal points move further away from the real $\boldsymbol{Re(k)}$ axis and closer towards the negative $\boldsymbol{Im(k)}$ axis, as the imaginary component of the potential $\boldsymbol{V_I(r)}$ becomes more negative. This trajectory indicates the presence of very broad resonances with shorter lifetimes. That is as the imaginary component of the potential $|\boldsymbol{V_I}|$ increases, sub-threshold resonances are observed.

These results correspond with those found in the literature review [9] [15] [18]

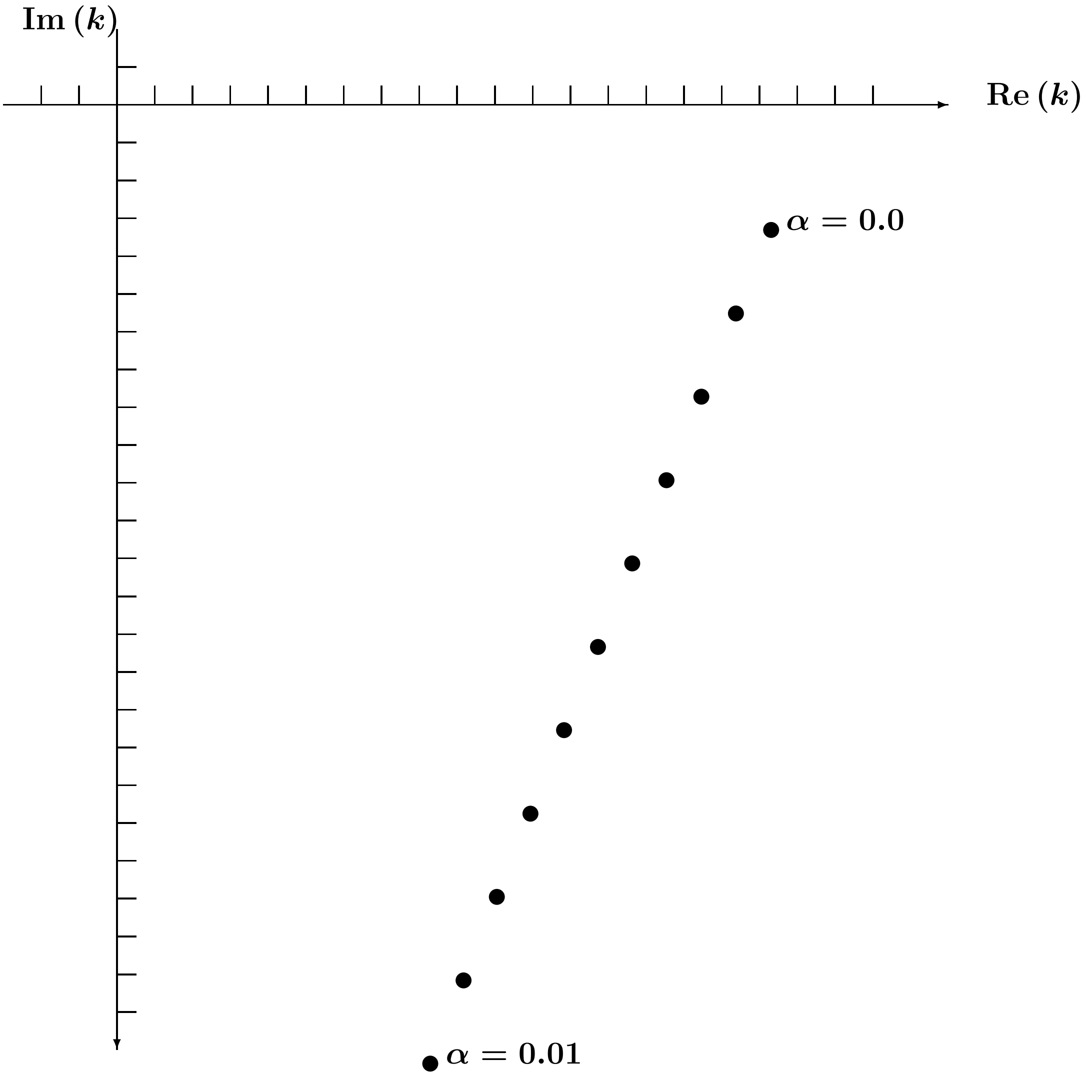

Figure 18: Plot of Spectral Points when $\boldsymbol{0 < \alpha < 0.01}$, ie, an increasing negative imaginary component of the potential

Recalling that

$$\boldsymbol{k^2 = \frac{2\mu E}{\hbar^2}}$$

it implies that

$$\boldsymbol{E = \frac{\hbar^2}{2\mu}\Big\{(Rek)^2 - (Imk)^2 + 2i(Rek)(Imk)\Big\}}$$

the values of $\boldsymbol{Im(k)}$ and $\boldsymbol{Re(k)}$ of the computation above can be substituted in the equation above to obtain the resonant energy $\boldsymbol{E_{res}}$.

Since

$$\boldsymbol{E_{res} = E_r + E_i} \quad \text{where} \quad \boldsymbol{E_i = -i\Gamma/2}$$

the width of the resonance window $\boldsymbol{\Gamma}$ can be determined In fact

$$\boldsymbol{\Gamma = -2\Big\{\hbar^2/\mu(Rek)(Imk)\Big\}}$$

Therefore, as the absolute value of the imaginary component of the central potential $\boldsymbol{|V_I|}$ increases, i.e, $\boldsymbol{\alpha}$ increases from $\boldsymbol{0}$ to $\boldsymbol{0.01}$, the $\boldsymbol{|Im(k)|}$, absolute value of imaginary component of momentum increases. Hence the value of $\boldsymbol{\Gamma}$, i.e, the width of the resonance increases. This implies energy can leak out faster and the resonance decays rapidly.

Alternatively, the half-life of the resonance

$$\boldsymbol{\tau_{1/2} = \frac{\hbar \ln 2}{\Gamma}}$$

becomes smaller as $\boldsymbol{\Gamma}$ increases. The lifetime is thus shorter and there is a rapid resonance decay.

Theoretically, there is a certain minimum energy that is required for collision or scattering to occur giving rise to quantum resonances. This minimal energy is the threshold energy and on the complex $\boldsymbol{k}$- plane, it lies on the diagonal line where $\boldsymbol{Re(k) = Im(k)}$.

As explained previously, when a collision occurs, it gives rise to different outcomes expressed as different channels. Each of these channels has a specific threshold energy. Subthreshold resonances are those that occur when

$$\boldsymbol{Re(k) < Im(k)}$$

which is below the diagonal where the threshold energy lies.

In this thesis, it is evident that as $|\boldsymbol{V_I}|$ increases, sub-threshold resonances are obtained. That is, broad resonances occur as a result of the increasing *absorptive potential*.

The following graphs show the trend in the resonance values, i.e, the zeroes of the Jost functions as the $\boldsymbol{\alpha}$ value of the imaginary component varies.

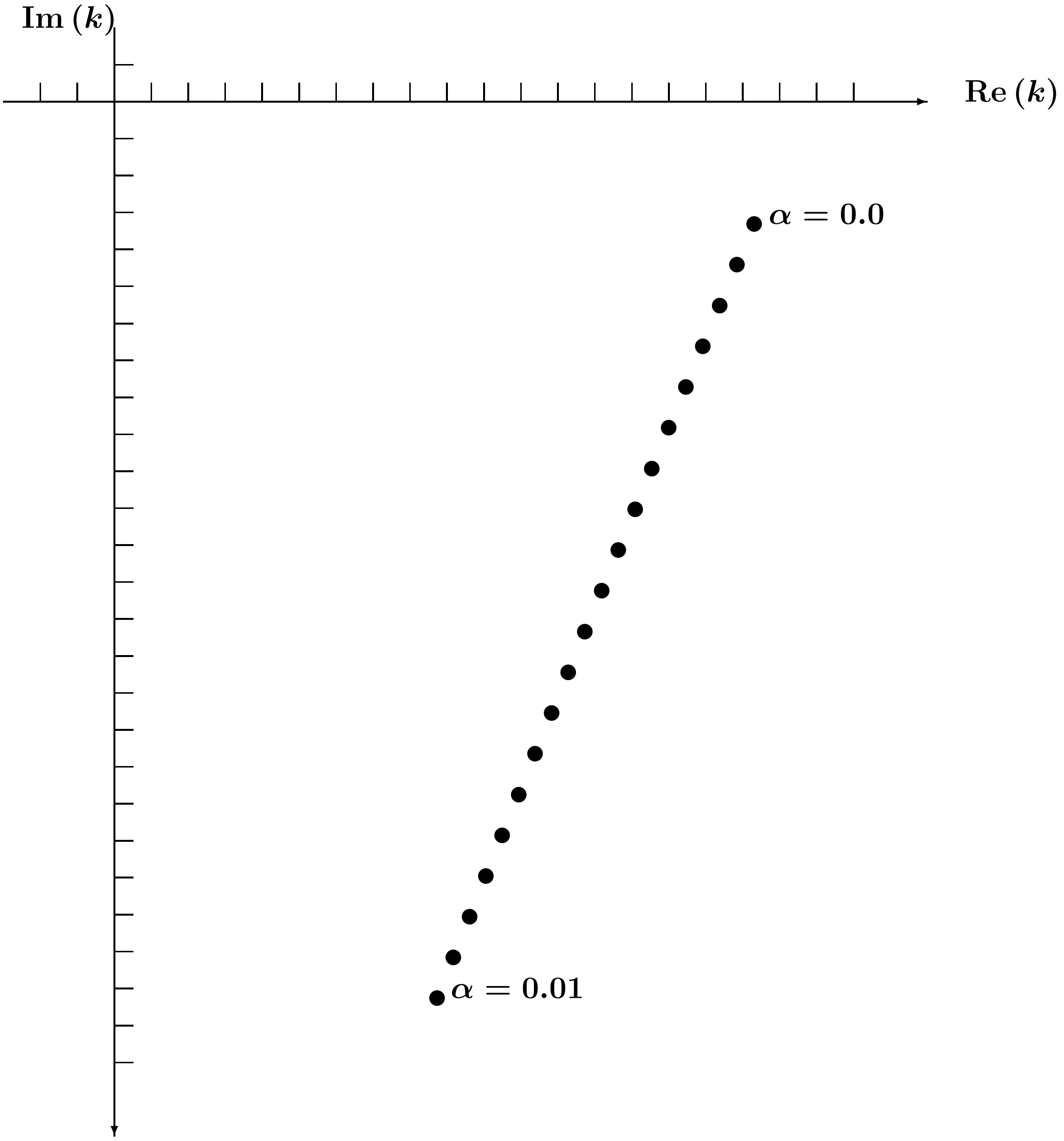

This is the plot of spectral points for $\boldsymbol{0 < \alpha < 0.01}$, i.e., the negative imaginary component, $\boldsymbol{Im(V)}$, is getting more negative.

The following graph illustrates the downward trend for two different resonances.

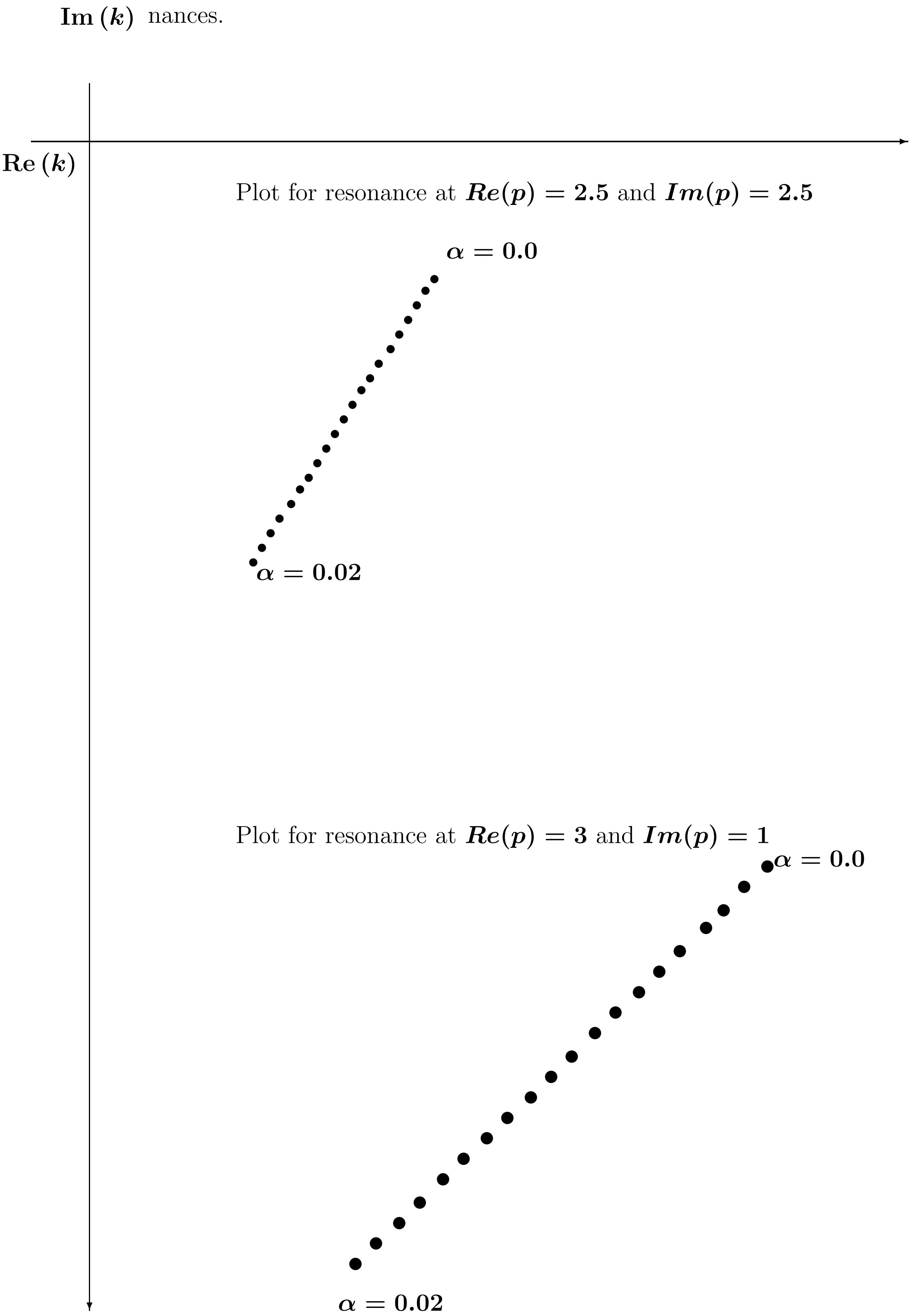

5 Conclusion

The postulates of quantum mechanics require that all observable physical quantities are described by hermitian operators. One of the reason for such a requirement is the fact that all the eigen-values of hermitian operators are real. When we deal with Hamiltonians, this means that the energy is real. In many cases, however, it is convenient to allow the energy variable to have complex values. In particular, the quasi-bound (or resonant) states are defines as the spectral points of the Hamiltonian at complex energies. Due to the presence of the imagginary part in the energy, these states become non-stationary, i.e., the time- dependent exponential factor in the wave function diminishes with time. One way to locate such complex eigen values of a Hamiltonian is the method of complex rotation of the coordinate (which we use in our calculations). As a result of such a rotation, the Hamiltonian becomes non-hermitian.

Another case when it is convenient to deviate from the requirement of hermicity, is an approximate treatment of multi-channel systems, when only one, the most important channel is considered explicitly, while the presencce and influence of all the other channels are simulated by an imaginary part of the interaction potential. The Hamiltonian with a complex potential is non-hermitian and does not conserve the number of particles. The particles from the explicit channel disappear when they transit into any of the implicit channels.

Complex potentials are called optical potentials, by analogy with classical optics where the absorption of light can be simulated by introducing complex refractive index. Originally, optical model was introduced around 60 years ago in the theory of nuclear reactions. Since then it found vast applications not only in nuclear physics but also in atomic, molecular, solid state and particle physics. The idea of reducing a multi-channel problem to an effective single-channel one by simple introduction of an imaginary part of the potential turned out to be very attractive and beneficial. However, the optical model was mostly used in calculations of the scattering processes. When it comes to dealing with resonances, the model finds itself on shaky grround. The difficulty stems from the fact that in this instance, there are two types of non-hermicity: one due to the complex part of the potential, and the other due to the complex eigen values of the Hamiltonian.

In the present thesis, one aspect of the difficulty associated with the application of the optical model to locating resonances, is clarified. Using a model optical potential, it is shown that the presence of the imaginary part in the potential causes the resonance spectral points to move towards and into the sub-threshold domain of the complex energy surface. To those who deal with resonances within the optical model, this result gives an indication and a guide as to where the resonances could be found and how their widths are modified by the implicit channels.

References

[1] R E D Bishop: Vibration, Cambridge university press, New York, 1965.

[2] A P French: Vibrations and Waves. M.I.T. Introductory Physics series.

[3] N Zettili: Quantum Mechanics, Concepts and Applications, Wiley, 2007.

[4] F Nunes: Elastic Scattering in Complex Potential

[5] J Al Khalili: Quantum; A Guide for the Perplexed

[6] J Simons: The Siegert Method in Resonance Scattering: Relation to $\boldsymbol{L^2}$ Methods, International Journal of Quantum Chemistry Vol.XX.779-780 (1981).

[7] K S Krane: Introductory Nuclear Physics, Wiley, 1988.

[8] J M Cassels: Basic Quantum Mechanics, 2nd edition, MacMillan Press London.

[9] PHY703 Quantum Mechanics, Lecture 5: Three dimensional Problems by Professor Rakityansky, UP.

[10] E W Swokowski: Calculus with analytic geometry, 3rd edition.

[11] PHY703 Quantum Mechanics, Lecture 8: Three dimensional Problems by Professor Rakityansky, UP.

[12] N Moiseyev : *Physics Reports* 302 (1998) 211-293.

[13] S Rakityansky and N Elander :Analysis of Individual Resonance Contributions to Two-Channel Scattering. *South African Journal of Science* 102, Jan/Feb 2006.

[14] S A Sofianos and S A Rakityansky: Exact method for locating potential resonances and Regge trajectories. 1996.

[15] A D Alhaidari: Studying resonance in the complex charge plane. Physics Dept, King Fahd university, Saudi Arabia.

[16] S A Rakityansky; Jost functions in quantum mechanics, November 2007.

[17] H Masui and Y K Ho: Resonance states with complex absorbing potential method, April 2002.

[18] J Zapata et al: Comparison method for scattering off complex central potentials, 1998.

[19] S Rakityanski: Quantum Mechanics Exam Nov2010

[20] Mott N F and Massey H S W 1965: The Theory of Atomic Collisions

[21] Joachim C J: Quantum Collision Theory

[22] R Marriot, D Micha: Physics Review 180 120, 1969

[23] R Resnick, REisberg et al :Quantum Physics of Atoms, Molecules, Solids, Nuclei and Particles.

[24] PHY703 Quantum Mechanics, Lecture 4: Time evolution, Conservation laws, Corresponding principle.

[25] PHY703 Quantum Mechanics, Lecture 10: Approximate Methods.

[26] Swokowski: Calculus, Wiley.

[27] PHY703 Quantum Mechanics, Lecture 8: Three dimensional Problems by Professor Rakityansky.

[28] physics.uwyo.edu/QM/lecture11 by Prof Lev Deych: Schrödinger Equation in spherical coordinates, Angular momentum.

[29] PHY703 Quantum Mechanics, Lecture 7: Angular momentum by Professor Rakityansky.

[30] George B Arfken, et al: Mathematical Methods for Physicists, 7th edition

[31] B Josephson: Lecture 2; Quantum Mechanics in one dimension,Cambridge University.

[32] V D Skarzhinsky et al: Singular Potentials and Absorption Problem in Quantum Mechanics, 2004

[33] F Nunes: Elastic Scattering in Complex Potential

[34] Goethe University: Lecture 6; Scattering Theory, Partial Wave Analysis.

[35] S A Rakityansky: Jost functions in quantum mechanics, Department of Physics, University of South Africa, November 2007

[36] Swokowski: Calculus, Wiley.

[37] S A Rakityansky: Jost functions in Quantum Mechanics, Physics Department, University of South Africa, November 2007